Journal of South American Earth Sciences 106 (2021) 103066

Contents lists available at ScienceDirect

Journal of South American Earth Sciences

journal homepage: www.elsevier.com/locate/jsames

The glacial paleovalley of Vichigasta: Paleogeomorphological and sedimentological evidence for a large continental ice-sheet for the mid-Carboniferous over central Argentina

Victoria Valdez Buso [a,*], Juan Pablo Milana [b], Mercedes di Pasquo [c], José Espinoza Aburto [d]

[a] School of Geosciences, University of Aberdeen, Aberdeen, AB24 3UE, Scotland, United Kingdom
[b] CONICET. Facultad de Ciencias Exactas Físicas y Naturales, Universidad Nacional de San Juan, Av. Ignacio de la Roza 590 (O), San Juan, CP 5400, Argentina
[c] Laboratorio de Palinoestratigrafía y Paleobotánica, CICYTTP-CONICET-ER-UADER, Dr. Materi y España S/N, Diamante, E3105BWA, Entre Ríos, Argentina
[d] Universidad de Atacama, Avenida Copayapu 485, Copiapó, Chile

ARTICLE INFO

Keywords:
Paganzo basin
Late paleozoic glaciation
Guandacol Fm
Palynology
Digital elevation models

ABSTRACT

We present new data on the Vichigasta Carboniferous paleovalley, a glacial trough crucial to understand the type of glaciation that affected western Gondwana during the Late Paleozoic Ice Age (LPIA). The filling of this paleovalley starts soon after the mid-Carboniferous glacial peak. Stage I represents pro-glacial lacustrine deposits with outwash, glacially rafted dropstones, mass transport deposits (MTDs) and turbidites of the trunk and a lateral tributary valley. Base-level drop created the scenario for Stage II outwash deltas and sandur deposits, with westward flow. Stage III represents a flooding at the base of the Bashkirian, characterized by typical transgressive dark shales and distal turbidites. Stage IV represents a highstand prograding turbidite wedge. We worked in a detailed terrain analysis, surveyed the scarce sedimentary record left and recovered a rich palynoflora from mudstones of Stage 3. The almost complete erosion of the fill allowed us to analyze the shape of this paleovalley and compare it to Olta and Malanzán ones. Vichigasta and Malanzán paleovalleys show similar size, a clear U-shape and regular and homogeneous width downslope, a requisite for bypass glacial paleovalleys carved in a subcrop of homogeneous composition (basement), which allow us to interpret them as outlet valleys. Olta paleovalley ranks as tributary as its capacity is only one-third of the others. We also identified a basement high over the Vichigasta valley floor that suggests the presence of a potential drumlin supporting our interpretation as a bypass glacial valley. This post-glacial flooding event is widely observed at other glacial valleys as the Olta-Malanzán herein analyzed and others like Las Lajas and Quebrada Grande. The new data from Vichigasta paleovalley reinforce the hypothesis of a large ice-sheet located to the east of the craton.

1. Introduction

The Late Paleozoic Ice Age (LPIA) represents the longest Phanerozoic glacial interval (Veevers and Powell, 1987; Frakes et al., 1992) and comprises diachronous episodes of glacial and non-glacial conditions across the Gondwana supercontinent (Eyles, 1993; López-Gamundí, 1997; Isbell et al., 2003; Fielding et al., 2008; Gulbranson et al., 2010). Several works about the timing, extent and type of glaciation that affected Western Gondwana were published in the last decade (López-Gamundí and Buatois 2010; Isbell et al., 2012; Montañez and Poulsen 2013; Limarino et al., 2014; (Valdez et al., 2019; 2020, among others). A discussion about the type of glaciation that affected this region of western Argentina persists to date. While some authors suggest a large glacial event of the sort observed in North America, or Scandinavia, other authors suggest the glacial centers were only located near the western margin, as hypothetical mountain-shadow small glacier systems, and suggested that alternatively considered glacial valleys as the Malanzán, are in fact, non-glacial (Andreis et al., 1986; Azcuy et al., 1987; Moxness et al., 2018; Pauls et al., 2019).

One of the best places to evaluate the type of glaciation that affected the western margin of Gondwana during the LPIA is the Western Argentina. Innovative information on the LPIA, new stratigraphic, sedimentologic, paleogeomorphological and palynological data from the Carboniferous Vichigasta paleovalley is presented. It lies in the eastern Paganzo Basin (Fig. 1 A and B) and it has been recognized in early works of this basin (Limarino and Gutierrez, 1990; Astini, 2010),

* Corresponding author.
E-mail address: victoria.valdezbuso@abdn.ac.uk (V. Valdez Buso).

https://doi.org/10.1016/j.jsames.2020.103066
Received 22 May 2020; Received in revised form 24 November 2020; Accepted 25 November 2020
Available online 8 December 2020
0895-9811/

but any stratigraphic study was attempted until today. However, this locality may contribute to shed light on the controversy of the type of glaciation that predominated in central-western basins of South America during the LPIA. Two main interpretations are postulated: a) alpine glaciers emanating from a Paleo-Precordillera roughly coincident with the modern Precordillera (Amos and Rolleri 1965; Rolleri and Baldis 1969; Limarino and Spalletti 2006; Limarino et al., 2014), and b) a larger continental ice-sheet to the east (Sterren and Martínez 1996;

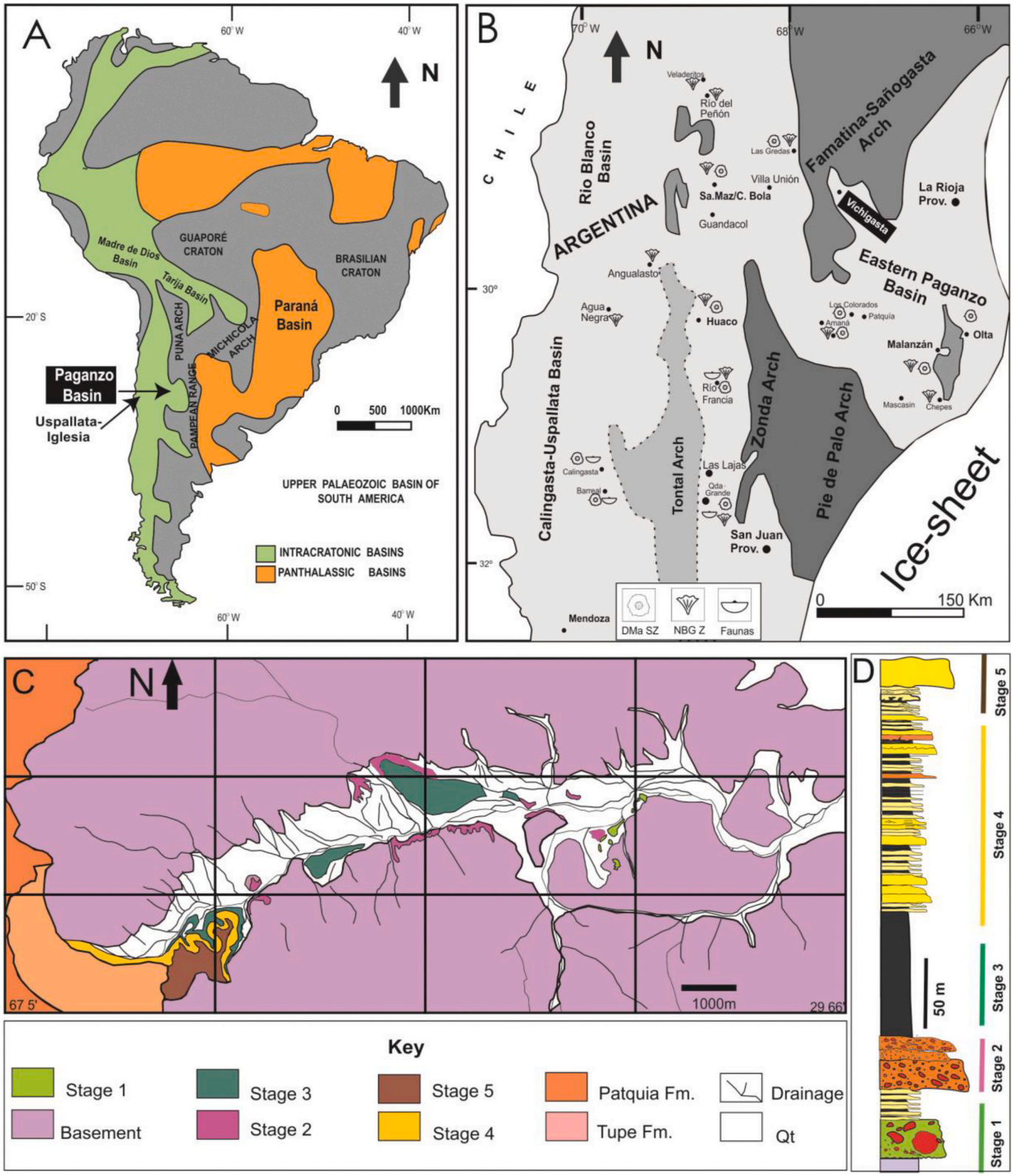

Fig. 1. A) Paleogeographic map of South America. Paganzo and other Paleozoic basins. B) Paganzo basin, the study area of Vichigasta and others cited in this contribution as Malanzán and Olta paleovalleys. The map also shows the distribution of the DMa Subzone, NBG zone and the faunas across the basin (modified from Azcuy et al., 2000, see supplementary online material). C) Geologic map of Vichigasta paleovalley and D) Stratigrafic column.

Kneller et al., 2004; Astini et al., 2009, 2010; Aquino et al., 2014; Socha et al., 2014; Valdez et al., 2017, 2020).

As recently suggested, the fill of the Malanzán paleovalley, a critical locality for the Carboniferous glacial history of South America, was not glacial in origin (Moxness et al., 2018; Pauls et al., 2019). Although, there are a plethora of papers suggesting the contrary (Sterren and Martínez, 1996; Enkelmann et al., 2014; Rabassa et al., 2014; Socha et al., 2014). The sedimentological and palaeontological information presented in this contribution allows us to discuss the original hypothesis of a large ice-sheet feeding glaciers that carved these valleys in the light of the recent non-glacial hypothesis. It is also important to note that the suggested alpine glaciation to the west is based on the presence of a hypothetical mountain chain (the Protoprecordillera) that was cutting the humidity flow to the east (continent interior) like the effect of Andean Range today. However, the presence of the Protoprecordillera is under debate and without it, this mountain shadow effect should be revised. The arguments supporting the absence of such a mountain chain have been recently discussed by Milana and Di Pasquo (2019 and references therein). Numerous information on sensitive climatic indicators (e.g. diamictites, coal deposits, fossils, content of organic matter) are widely used in paleoclimatic reconstructions (see Scotese et al., 2014). In Argentina, since the first studies carried on in the Pennsylvanian of the Paganzo basin, these indicators were recorded in different east-west localities (see Azcuy et al., 2000; Césari et al., 2007; Limarino et al., 2014, and references therein). In fact, an opposite gradient of humidity (increasing humidity eastwards) could be inferred based on the extent of coal seams and plant deposits in the eastern Paganzo Basin, which contrast to more recent interpretations (cf. Pauls et al., 2019).

In order to strengthen our hypothesis about the type of glaciation affecting the western Gondwana we have compared our results from the terrain analysis done at Vichigasta with those of the Malanzán and Olta paleovalleys. We demonstrate the paleogeomorphological link between the Vichigasta and Malanzán glacial paleovalleys despite being about 160 km apart (Fig. 1B). Under the ice-sheet hypothesis, both paleovalleys would have been probably draining the same ice body and hence, inheriting similar boundary conditions to transport ice to the Western Paganzo basin.

2. Local geology of Vichigasta

The Vichigasta locality has been mentioned by some authors (Limarino and Gutierrez, 1990; Astini 2010), but no detailed work has been reported. The first part of the valley is clearly modern due to its V-shape. There are some mentions of a possible glacial origin for this paleovalley (Astini, 2010), but no detailed study supported this interpretation. Thus, we surveyed the distinguishable late Paleozoic units present in this paleovalley that trends east to west (see Fig. 1C).

The sedimentary succession is not be observed in a single section, but the processes involved in the excavation and filling of the valley are interpreted from several partially disconnected outcrops. As shown later, Stage 1, which comprises the most relevant evidence for glacial depositional activity, was completely removed from most of the main valley during the subsequent Carboniferous filling. Stage 1 exists now as an erosional remnant preserved where sheltered from the main ice flow, in that we believe is a tributary valley engulfing. Therefore, the stratigraphic column (Fig. 1D) presented herein is composed of the observations obtained at several disconnected outcrops during field works carried out in the last part of 2019. Fortunately, in all cases it was possible to observe the preserved contacts between stages.

Our study focused on the Guandacol Formation known to be late Serpukhovian-early Bashkirian, confirmed by the first palynologic elements presented in this work. The local name of Lagares formation suggested in this area (Azcuy, 1970; Di Paola 1972; Morelli et al., 1984; Net et al., 2002, among others) is placed aside to unify terms across the Paganzo basin domain for similar depositional systems and vertical sequences to avoid the proliferation of formation names that describe the same unit. In fact, the similarity is striking between the Vichigasta succession and those ascribed to Jejenes or Talacasto formations (among many others) deposited in paleovalleys flooded by the same postglacial eustatic rise (cf. Valdez et al., 2020 and references therein). Thus, we recommend calling Guandacol Formation to the lower section at Vichigasta. We did not include in this study the analysis of the upper sedimentary successions, also attributable to the Carboniferous, probably ascribed to the Tupe Formation. The local late Paleozoic succession culminates with red beds typical of the Patquía Formation.

3. Methods

The study is focused on three lines of work: 1) physical stratigraphy and sedimentology, 2) terrain analysis and 3) paleontology. The first part of the work is centered on outcrop descriptions, using conventional techniques of facies analysis. Disconnected outcrops were described and mapped. For facies characterization and vertical stacking of stratigraphic levels, a geological log is shown at 1:250 scale (Fig. 1D). The stratigraphic analysis allows the recognition of four main stages described below. Parallel to this, a terrain analysis of this paleovalley and other related ones was carried out. During the fieldwork, a dark shale unit (Stage 3) was sampled for spore-pollen biostratigraphic analysis. Ten samples, named in the field M1-M8 and B1 and B2 and one shale of Stage 1 (repository numbers CICYTTP 2337–2347) were collected.

3.1. Terrain analysis

Terrain analyses were performed by extracting the best-detailed DEMs (digital elevation models) for the Vichigasta and also Olta and Malanzán paleovalleys. Considering that we looked for the highest resolution, we used a DEM of 12.5 m pixel size produced out of the ALOS-PALSAR sensor. Due to the distance between DEM of the studied areas, we use a different satellite image for each one: 1- AP_21946_FBS_F4220_RT1 for Vichigasta, 2- AP_21414_FBS_F6560_RT1 for Olta valley, 3- AP_27030_FBS_F6560_RT1 for the Malanzán valley together with the AP_21414_FBS_F6560_RT1 used for Olta. Geographical Information System tools were used to remove erroneous values in DEM, and incorrect values were populated with statistical information. Once having the adjusted DEM, the position of the different profiles was set, limiting the start and end of each profile. The profiles were taken from the peneplain or moderately eroded shoulder. Each profile matched to the other when the upper slope decreased from to 20-22° of inclination. Three profiles were obtained for Malanzán and Olta and four for Vichigasta that shows a larger downslope development, and are depicted in distance vs. height as the final result. Dataset used was ASF DAAC 2019, ALOS PALSAR_ Radiometric Terrain Corrected high resolution. Includes Material from ©JAXA/METI 2011 and PALSAR Radiometric Terrain Corrected high res 10.5067/Z97HFCNKR6VA. Terrain data available on request to the authors.

3.2. Palynologic study

Samples were processed at the Laboratory of Palynostratigraphy and Paleobotany of the Centro de Investigaciones Científicas y Tecnológicas de Transferencia a la Producción (CICYTTP-CONICET-ER-UADER) at Diamante, Entre Ríos. A standard methodology of maceration with HCl and HF was applied to obtain organic residues that were observed preliminary to discard the barren ones and to decide the following steps to improve those productive. At this step, slides were mounted with jelly glycerine. Five productive residues needed a second time of HF to eliminate most of the remnant quartz and after neutralization with distilled water, boiled in HCl, washed and sieved through a mesh of 25 μm and mounted this time with Trabasil (Noetinger et al., 2017). Palynological analyses performed using a light microscope Nikon E200 with a video camera Amuscope 14 Mp. Palynologic slides and residues

cataloged with specific acronyms and numbers corresponding to the collections housed at CICYTTP-CONICET-ER-UADER (di Pasquo and Silvestri, 2014). Sedimentary organic matter (palynomacerals) of the kerogen types here identified are in agreement with Tyson (1995) and Batten (1996) as follows: phytoclasts (tracheids, cuticles), opaques (non-structured brown and black debris), amorphous organic matter (AOM), and palynomorphs. Quantitative (c. 250 specimens of palynomorphs per sample) and geo-stratigraphic distribution of species (with their authorities) and illustration of selected species addressed below.

4. Results

4.1. Lithostratigraphic analysis of the valley fill

Stage 1: Proglacial sediments.

This stage is composed of three units (A, B and C) and is the oldest recorded in this valley. It crops out locally and only preserved in a limited area of the southern margin of the paleovalley in its eastern section (see Fig. 1B). The unit is absent in other places and is interpreted to have been eroded by the action of the coarse-grained fluvio-alluvial systems of Stage 2.

Unit A- *Thin-bedded sandstones and siltstones with outsized clasts*: this unit is up to 10 m thick and consists of alternations of siltstones and sandstones, with clasts that range from millimeters to decimeters in size. Out-sized (up to 100 cm) rounded, sometimes faceted or striated clasts of granitic composition are also present. The fine-grained facies are disposed in heterolithic fine to medium-grained beds where some intervals show abnormal clast concentrations that disrupt bedding, also causing bending and rucking structures at lateral contacts between bedding and largest clasts. (Fig. 2A–C).

Unit B- *Medium grained-bedded sandstones and siltstones with outsized clasts*: this unit is up to 12 m thick and consists of the alternations of fine to very fine-grained sandstones and siltstones. Tabular sandstones beds of several centimeters thick represent the lower section of the unit. The base of some beds shows loading and flame structures. Thinner beds are massive, normally graded and show parallel lamination. Outsized clasts occur in the siltstone intervals that separate the sandstone facies (Fig. 2D). The upper part of the unit shows local syn-sedimentary deformation, such as contorted beds contained within decimetre-scale slumps.

Unit C- *Massive diamictites*: This deposit consists of a silty/muddy matrix with basement clasts of various sizes (up to 60 cm) and preserves syn-sedimentary deformation such as folding and thrust faults. Horizontal thrust faults can be easily detected across the outcrop (Fig. 3) showing displacement direction from east to west (in the original downstream direction of the paleovalley). In addition, blocks of about 7 m long of fine-to coarse-grained sandstone appear randomly in the silty matrix. (Fig. 3). As shown by the interpretation of the mosaic, these diamictites are thickest in the middle of the outcrop and fringes in both eastern and western directions.

Interpretation.

Unit A is interpreted as ice rafting and gravity flows deposits. The disrupted beds (bending and rucking) are unequivocal examples of ice rafting drop and ground impact effects, as they are diagnostic features caused by the impact of the outsized clasts (Thomas and Connell 1985). The medium grained-bedded sandstones (Unit B) are the results of turbidity currents, where massive texture and base-loaded sandstones represent fast sedimentation, and alternating parallel and ripple cross-lamination within individual beds of thin-bedded sandstones are the result of a fluctuating flow regime (hyperpycnal flows). Lastly, Unit C interpreted as a local mass transport deposit (MTD), possible coming

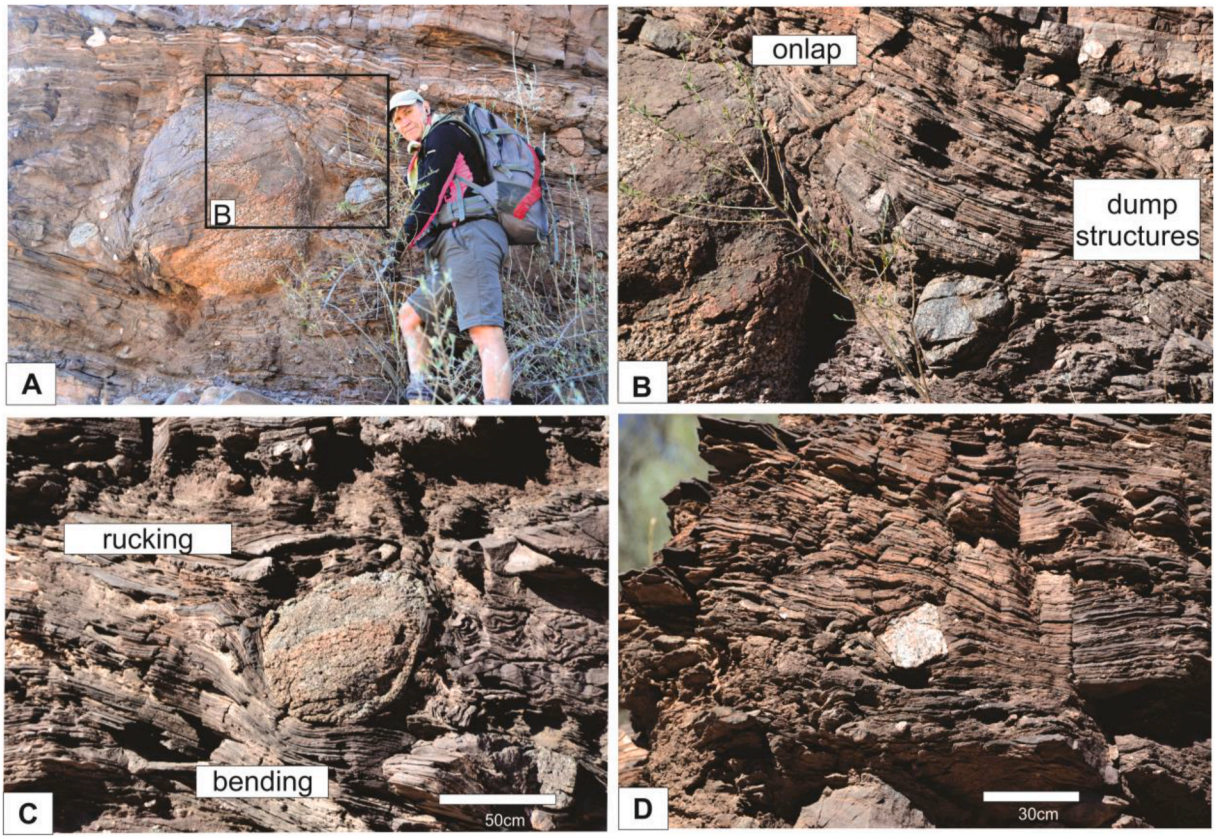

Fig. 2. Proglacial sediments of Stage 1. A) Outsized granitic dropstone of about 1m in size, person for scale. B) Onlap of the finer sediments onto the dropstone of figure A and dump structures. C) Rucking and bending structures at the base and top of the precambrian dropstone. D) Thin bedded heterolitics beds and an angular dropstone.

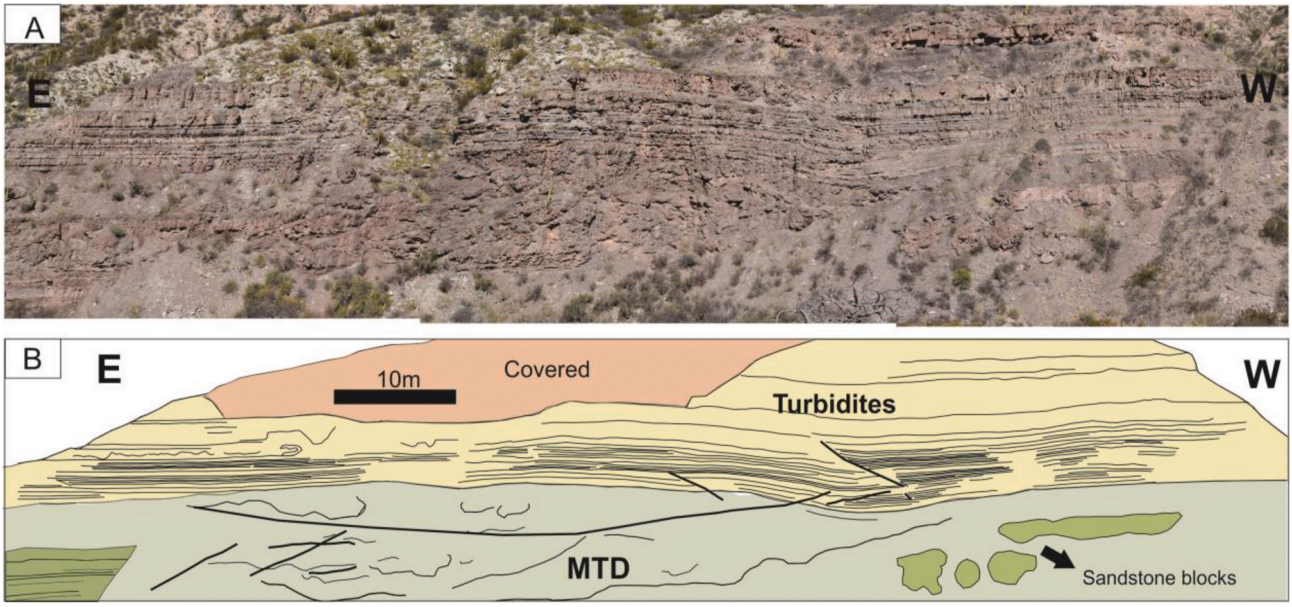

Fig. 3. A) Mass transport deposit (MTD) and medium-grained bedded turbidites in a lateral of the paleovalley. B) Photointerpretation showing the different faults (thicker lines) across the MTD and rafted sandstone blocks of about 7 m in size.

from the steep sidewall of paleovalley. This interpretation is based on the fact that this MTD unit (Fig. 3) thins out to the east and west, indicating that its flow line was towards the observer. However, we are not sure if turbidites associated were fed from the southern side of the valley, probably due to the effect of a tributary valley or along the trunk valley due to the fact directional structures are not very common. The unit was deposited in a subaqueous (possibly lacustrine) setting, with the dropstones indication floating ice, suggesting a pro-glacial glacial environment. Hence, pro-glacial sediments (IRD, Unit A) composed the Stage 1 and some gravity flows as turbidites (Unit B) and debris flows/slumps (Unit C) added material to the succession. Alternatively, the entire stage could be interpreted as an ice dammed lake, due to its particular position near to the walls of the paleovalley and slightly within a re-entrant of the valley side. No more outcrops of this stage appear into the valley center. A particular feature that draws our attention was the quasi-horizontal thrust within this unit (Fig. 3). No possible tectonic faulting would come into this unit due to the fact this kind of structure is not present in the basement that hosts the paleovalley fill. The fault in the MTD suggests push direction at 90° of the expected flow direction that emplaced the MTD, and thus in coincidence with the trunk valley strike and the interpreted glacier advance direction. We suggest this faulting may represent the effect of glacial pushing and hence a glaciotectonic feature.

Therefore, Stage 1 could be interpreted in two different ways: A) deposited as a unit associated with the main valley glacier, and hence it would probably require a glacier front very close to the location to justify the horizontal thrusting observed in the proglacial deposits. B) In the case of an ice-dammed lake, we would expect larger deformation on outcrops that are actively in contact with the flowing glacier, a fact not observed. We are inclined to the option A that would imply a terminal glacial position (for explaining the horizontal thrusting as it happens in push moraine) and a high water level to allow the IRD and turbidite suite observed. Finely laminated shales and other muddy facies in Stage 1 show evidence of oxidized horizons (palynological barren samples), whereas those shales of Stage 3 are not (palynological fertile samples), which might suggest a drop of base-level between Stage 1 and 3, and subaerial exposure of Stage 1. As shown below, the direct contact in many places of Stage 2 and the basement supports this interpretation.

Stage 2: Outwash deltas and sandur deposits.

This unit follows deposition after Stage 1. There are no clear stratigraphic relationships between Stages 1 and 2. However, Stage 2 concordantly underlies Stage 3 (via a fast transition, see Fig. 4A), so it is undoubtedly younger than Stage 1. A more careful revision of this locality may help to understand the relationship between Stage 1 and 2 that we interpret as a significant erosional surface. A re-advance probably caused the glacio-tectonism described in Unit C of Stage 1. However, continued fluvio-alluvial erosion during Stage 2 surely helped on cleaning up the valley of Stage 1 deposits, as Stage 2 almost everywhere lies directly over the crystalline basement. We found two main units as part of Stage 2:

Unit A. Coarse-grained fluvial and colluvial sediments: This coarse unit has a distinctive reddish color; and when present erodes all Stage 1 and where its base is observed, rests directly on the Pre-Cambrian basement. The coarsest grained deposits are mainly represented by clast-supported conglomerates intercalated with poorly-sorted pebbly sandstones, with random boulders 60–80 cm large. They show normal and inverse grading and low-angle cross-bedded. Clast-supported conglomerates and pebbly sandstones appear amalgamated in this unit. In the finer-grained parts (medium to coarse-grained sand), there are very fast changes in grain size suggesting a very irregular and pulsating discharge regime. The conglomerates of this association are oligomictic, and clast composition suggests a local derivation directly from the pinkish granitic basement that forms the subcrop of most of this valley. The clast size varies from pebbles to boulders, and the shape ranges from sub-angular to rounded. This association crops out at the margins of the paleovalley and eastern outcrops (Fig. 4A–C).

Unit B. Medium scale cobbly clinoforms: It is defined by packages of high angle pebbly to cobbly conglomerates reaching 3–4 m thick sets and are located in the deepest parts of the paleovalley. These conglomerates show clinoforms with steep (40°) and quite planar foresets that, in all cases, demonstrate progradation towards the west (Fig. 4D). Massive or chaotic sand-matrix-supported conglomerate (Fig. 4C) is also a representative facies of this unit, separating solitary clinoform sets in many cases. The shape of the clasts is angular to subangular; the matrix consists of the mixture of coarse-grained and poorly sorted sandstones and dark grey siltstones. Lenses of fine-grained sandstone appear deformed or distorted. Fine-grained facies as siltstones and mudstones of Stage 3 appear on top of this unit B or Unit A (Fig. 4A), suggesting a geographical control of the facies groups associated to the two main units of Stage 2.

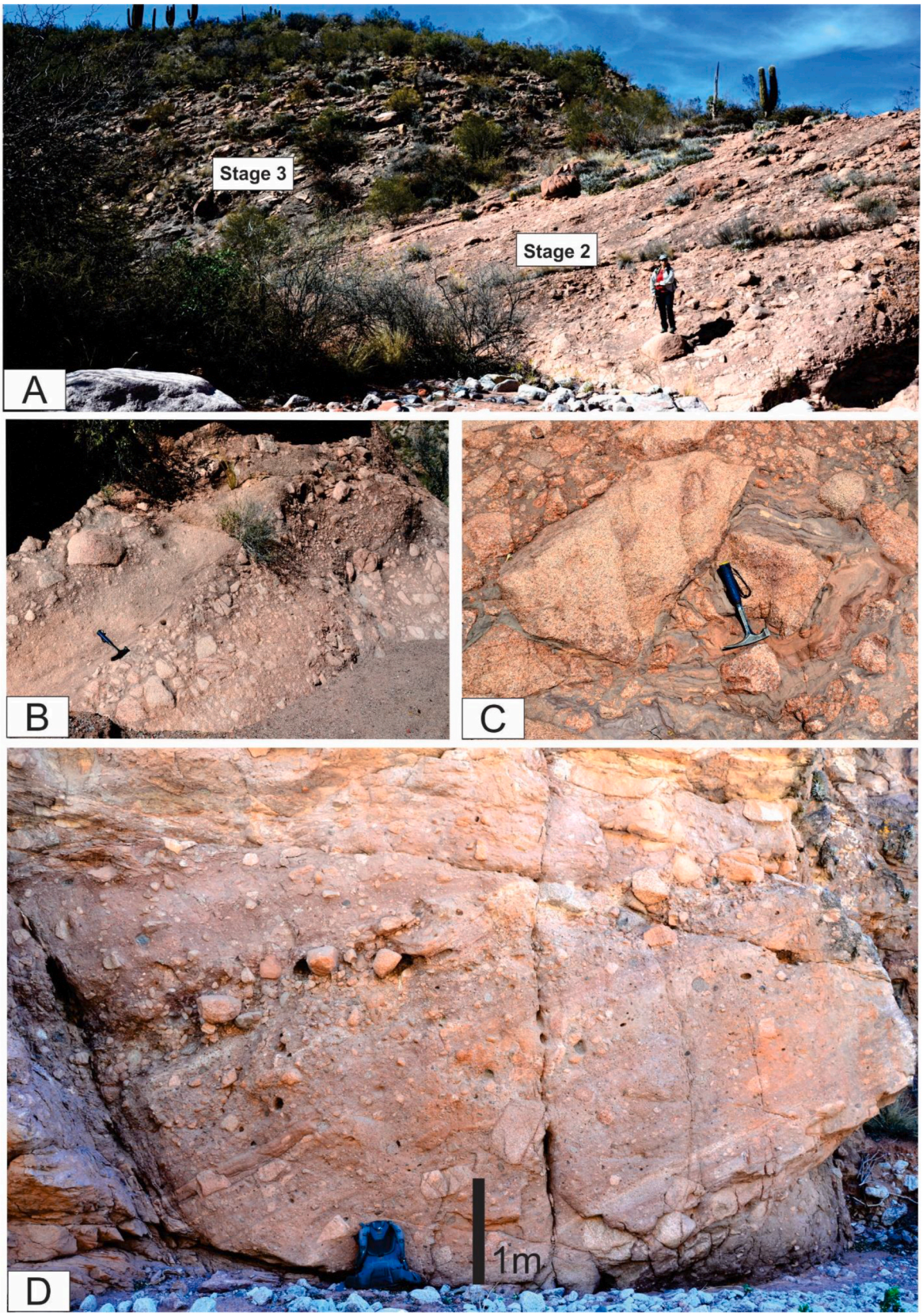

Fig. 4. A) Conglomeratic facies of Stage 2 overlaid by finer sediments of Stage 3. Person for scale. B) Inverse grading clast support conglomerates of Stage 2. Hammer for scale. C) Matrix supported conglomerates showing a massive texture. Hammer for scale. D) Clast supported conglomerates. Clinoforms and imbricated clast shows a paleotrend towards the west.

Interpretation.

This stage represents a base level drop as Unit A and suggests subaqueous deposition of buoyant plumes, floating ice and mass-gravity flows with a minor effect of fluvial outwash streams, whereas unit B is a dominant subaerial deposition with the exception of the progradation of small Gilbert deltas in localized ponds. The conglomerate and sandstone units are interpreted as being a result of deposition by a combination of processes that occur in a proglacial setting. The intercalation of massive and stratified, very poorly sorted and mostly coarse-grained deposits including pebbles to boulders suggest unsteady, high-energy discharge. At the margins, notably oligomictic poorly sorted boulder conglomerates of this Stage 2, suggest the supply of colluvial systems fed by the valley margin, also supporting a base-level drop. The coarsest deposits (Unit A) of amalgamated and low-angle cross-bedded facies represent typical features of a well-developed braided fluvial distributary plain (sandur) pointing to a proglacial outwash system. Such outwash deposits may extend for several kilometers, as they do in this paleovalley (see map, Fig. 1C). On the other hand, scarcity of Unit B deposits and very poorly sorted nature and ample grain-size range from boulders 50 cm large to fine-grained sand (Fig. 4D) considered in a context of well-defined clinoform, suggests the existence of some small (2–4 m deep), probably short-lived ponds that were rapidly filled by prograding medium-scale Gilbert deltas. These ponds are very common in outwash plains and in many cases are fostered by the melting of buried masses of ice, left during rapid glacial retreat. Both units indicate the same depositional system: a sandur or outwash plain, as ponds in this environment are quite frequent. The creation of ponds by buried ice melting is a very common process in the case of low-gradient valleys as a minor thermal change may cause melting of long segments of these low-gradient glaciers. Stage 2 appears on top of the basement even at expected deeper parts of the valley, so the previous Stage 1 was almost all eroded. The remnants of Stage 1 observed are interpreted to have been left as erosive remnants protected at valley side irregularities in a way of present-day fluvial terraces. This would explain how today, Stage 2 deposits seem to occur at topographically lower places with respect to Stage 1 deposits. As indicated before, the transitional pass from any of the coarse-grained facies of Stage 2 to the shales of Stage 3, via a fast flooding surface, leaves no doubt about the stratigraphic order presented here.

In summary, Stage 2 indicates a base level drop pointing this as a lowstand system tract bounded by two high-stand units.

Stage 3: Flooding of the paleovalley.

This unit is from up to 100 m thick (although in most outcrops it does not show its top) and overlies Stage 2 via a fast transition (Figs. 4A and

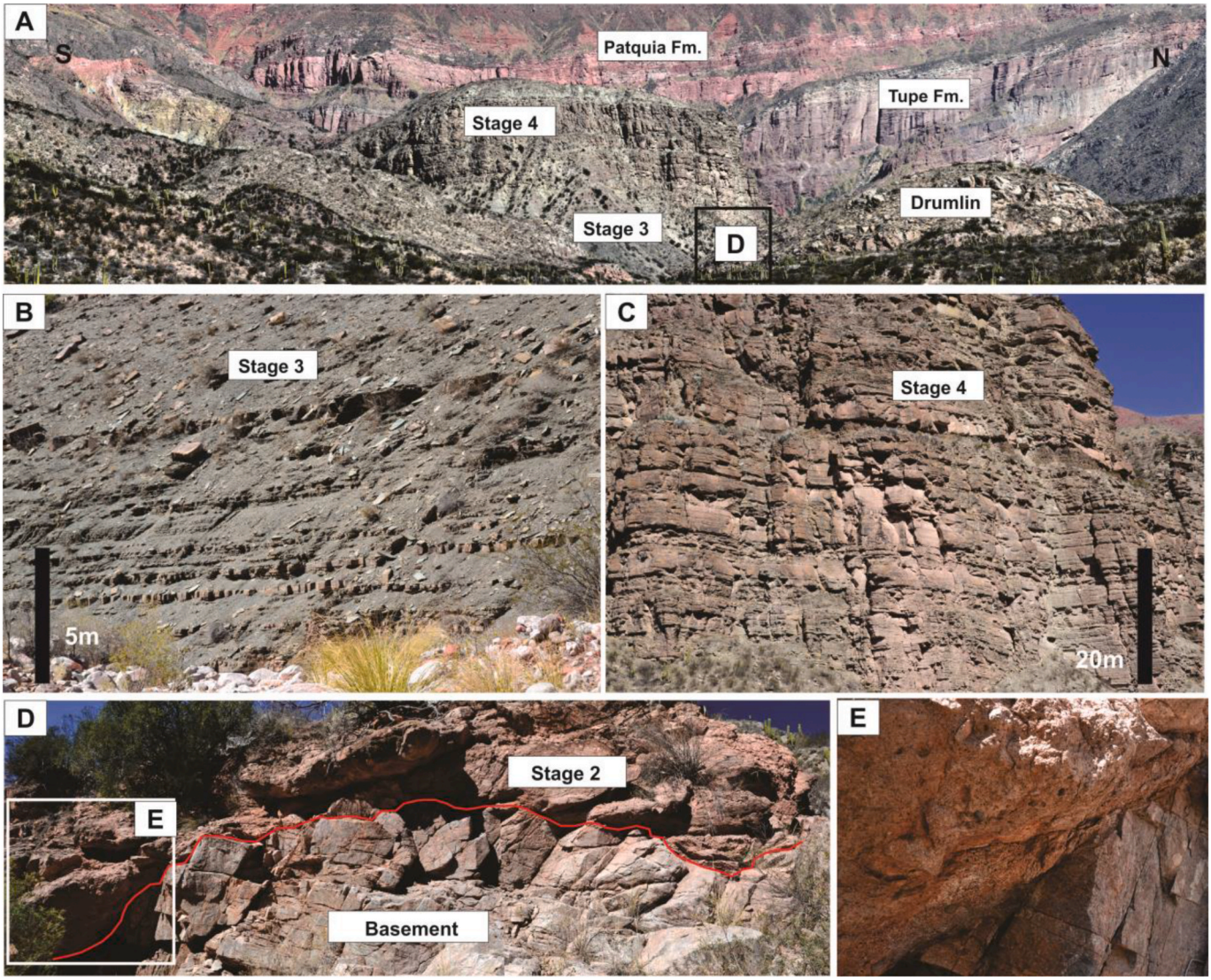

Fig. 5. A) Panoramic view of the paleovalley. At the centre Stages 3 and 4, at the back Tupe and Patquía formations. Also is possible to see a preserved paleodrumlin (right of the picture). B) Mudstones and distal turbidites of Stage 3. C) Sandy turbidites of Stage 4. D and E) Paleodrumlin and glaciar erosion of Stage 2.

5A). It consists of fine-grained sediments such as dark shales, very fine-grained sandstones and siltstones (Fig. 5B). Occasionally, marly levels were also found with cone-in-cone structures. The fine-grained sandstones appear as thin tabular beds at the base of the succession, ranging from 5 to 15 cm thick. Some beds appear normally graded with ripple cross-lamination at their tops. Some of them present a sharp base showing no erosional features. Massive fine to very fine-grained sandstones with loaded bases also occur. The middle part of the section shows some sparsely distributed medium-bedded tabular sandstones. Finally, the uppermost part of the section becomes more fine-grained, mainly represented by dark grey siltstones and mudstones. These facies can appear massive or parallel laminated.

Interpretation.

The tabular sandstones at the base of the unit were probably deposited by distal turbidity currents, while the siltstones and mudstones represent suspended sedimentation with a high rate of sediment supply. This entire interval represents the rapid flooding of the valley and the sedimentation during the transgressive and early highstand. This interval correlates with the widely recognized marine transgression recorded elsewhere in the basin (Limarino et al., 2002; Valdez et al., 2017, 2020).

Stage 4: Turbidite sheet lobes.

These deposits consist of a succession up to 200 m thick, forming packages from thin-to thick-bedded, normally-graded, massive sandstones, with thin mudstone or siltstone intervals forming the tops of the graded beds (Fig. 5C). The thinner beds are from 5 to 10 cm thick, with sharp bases, and consist of very fine-grained sand. Some beds have parallel and ripple cross-lamination. Medium-bedded sandstones are mostly tabular and comprise massive, plane-bedded and/or ripple cross-laminated sandstone with or without intervening mudstone. Some sole marks at the base of sandstones beds (mainly flutes marks) indicate paleoflow towards N/NW. The sandstones are organized in tabular packages, with one exception of a package of turbidites that wedges towards the north, suggesting it was deposited by northward-directed flows, and thus perpendicular to the valley axis.

Interpretation.

This succession of well-bedded sandstones, represents high to low density (massive/plane-bedded and ripple cross-laminated respectively), short-lived turbidity currents. Some sandstone beds with structures that indicate both waning and waxing behavior acting during a single deposition event were originated from hyperpycnal flows. Stage 4 represents the effect of progradation of the highstand wedge deposited after the main flooding interval. These packages of turbidites suggest the depositional system organized in sheet lobes, like many other postglacial turbidites in the Carboniferous (cf. Fallgatter et al., 2019). Most lobes were probably sourced from the main valley axis, although in one case, a lobe seems to be generated by flows entering from the south, as it thins towards the north within the main valley system.

4.2. Paleovalley shape analysis

In order to analyze the shape of the valley profile, we have undertaken a terrain analysis using processed DEMs (digital elevation models) for this paleovalley (see above). We also included the Olta and Malanzán paleovalleys in our analysis to understand the potential relationships between those well-preserved geomorphological features and the Vichigasta paleovalley. It should be taken into consideration that these geomorphological features have been modified by many processes such as: (a) the hill-slope erosion and fluvial erosion soon after the ice retreated, witnessed by the monomict character of the marginal colluvial-braided proglacial Unit A identified in Stage 2; (b) the subaqueous erosion during the transgressive process (Stage 3), (c) the marginal erosion during the development of the highstand turbidites (Stage 4), (d) a potential Mesozoic planation as suggested by Jordan and others (1989) for the large-scale basement peneplain elaboration, that might have reworked valley shoulders, (e) the Neogene to recent erosion by colluvial, alluvial, and fluvial processes. Additionally, the original valley profile is altered by the depositional remnant of both Late Paleozoic deposits, and sometimes seemingly thick Quaternary alluvial deposits.

For each of the conjectured glacial paleovalley mentioned here (Vichigasta, Malanzán and Olta), a larger area was extracted to produce a DEM (Fig. 6). This area included the valley shoulders (i.e. the intersection between the steeper valley margins and the upper peneplain, and including part of the peneplain), and the process and source data is indicated in the methodology section. After producing the DEM, transverse profiles were selected to represent better the original paleovalley profile, thus meaning profiles were located preferentially along ridges between modern tributaries to the main valley. In this way, we do not only avoid the effect of modern erosion of the basement, but also the depositional effect of the small alluvial fans formed at the foot of these drainages that protrude over the original valley profiles. However, it is clear that in many cases, the paleovalley has not been completely re-excavated to its original level as in Malanzán where Carboniferous fill still occupies the modern valley (Figs. 6 and 7).

4.2.1. Vichigasta paleovalley

Four profiles were constructed through this paleovalley in order to portray its shape (Fig. 6). The first observation is that the one located near the entrance is shallower and does not perfectly follow the shape of the other three. The immediate conclusion might be that this profile, which used to be upstream on the glacial flow, is now located downstream in the present alluvial flow and therefore, it has been subjected to a greater erosion (since the erosive process tends to increase downstream). However, we believe this difference is due to the original differences in basement composition. While the geological map indicates that the basement is composed of Ordovician granites, we could see in the field a difference between a darker grey basement in the eastern part of the paleovalley (profile 1) and a more pinkish-orange granite to the west. We suggest the differences in the competence of these different rocks might cause a difference in the erosive profile of this paleovalley. Many studies showed that glacial valleys adjust their size and profile to the type of rock composing the glacier's subcrop (Harbor, 1995; Augustunuz, 1995), and given the shared U-shape profile between profile 1 and the others, we interpret these differences are due to the different rock competence between these two sectors of the valley.

Unfortunately, the DEM does not include a large part of the peneplain as it was completely eroded in the east and because it is located quite far from the valley in the western parts. However, we detected a minor difference in the altitude of the peneplain (higher to the north) that is compatible with a c. 5° tilt to the south of the peneplain and thus, of the entire paleovalley. It adds to this, a subtle compactional syncline of the Carboniferous deposits, so beds on the southern side are horizontal, whereas those on the northern side reach dips of up to 10° S.

Due to the position of the shoulders, we can estimate that during maximum glaciation, the glacier attained 2.8 km in width and 700 m maximum depth, suggesting a potential ice section of 3.08 km^2. The similarity of profile shapes (with the exception of a minor variation to the profile 1) allows us to interpret that this valley was a conduit of glaciers. This is according to known models of glacier shape variations downstream, in which after passing the point of glacier flow concentration near the Equilibrium Line Altitude (ELA), the glacier width tends to be constant (Anderson et al., 2006). Note that the largest Alpine glacier (*Aletsgletscher*) is 1.5 km wide at its section of constant width and hence bypass. Therefore, a 2.8 km wide is a reasonable size for a glacier transporting ice out from a large ice-sheet. The morphological evidence extracted from the terrain analysis suggests that Vichigasta contained an outlet glacier moving large ice-volumes westwards.

4.2.2. Olta and Malanzán paleovalleys

The analysis carried over these two paleovalleys suggests that they did not form a single ice conduit as there are clear differences in size,

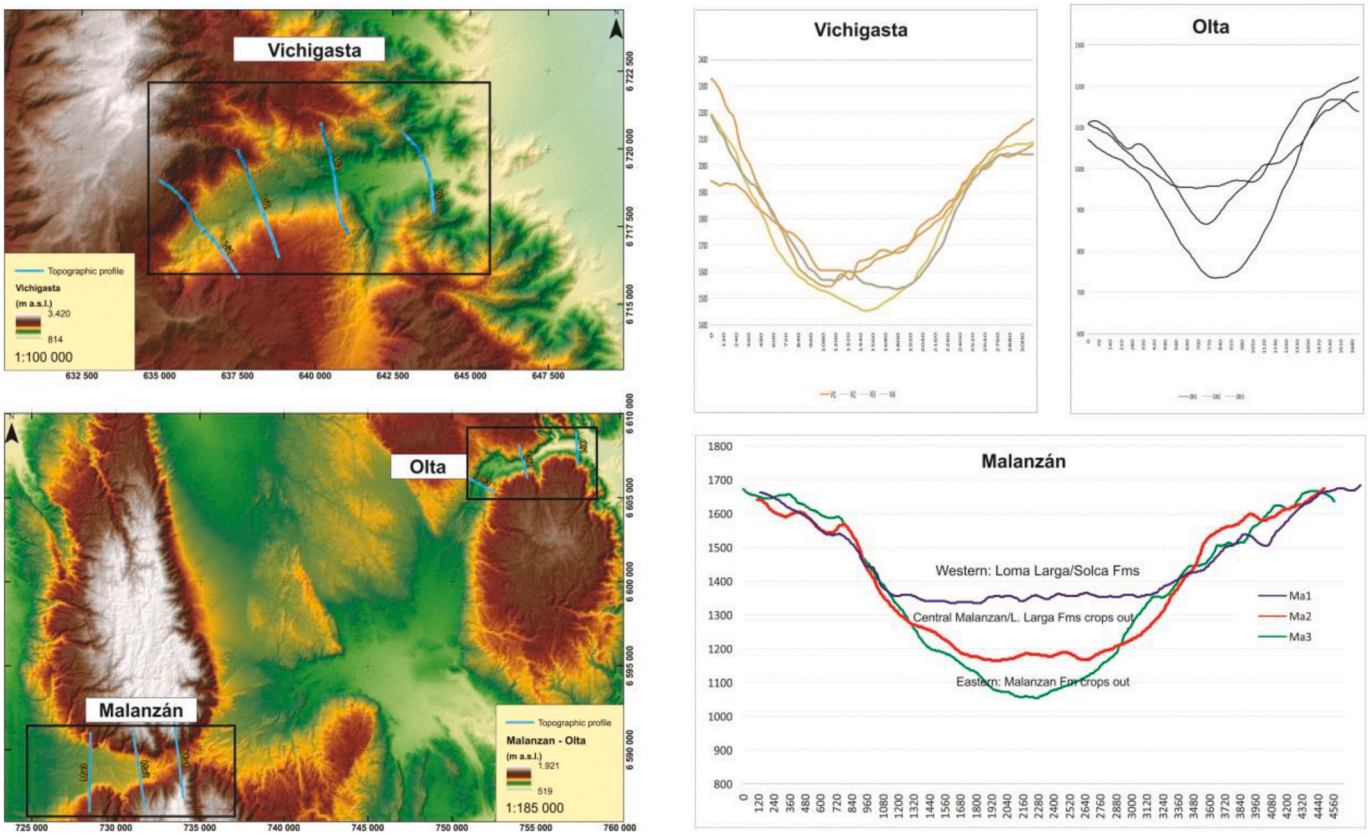

Fig. 6. Digital elevations models (DEMs) and the individual profiles obtained in this work for Vischigasta, Olta and Malanzán paleovalleys.

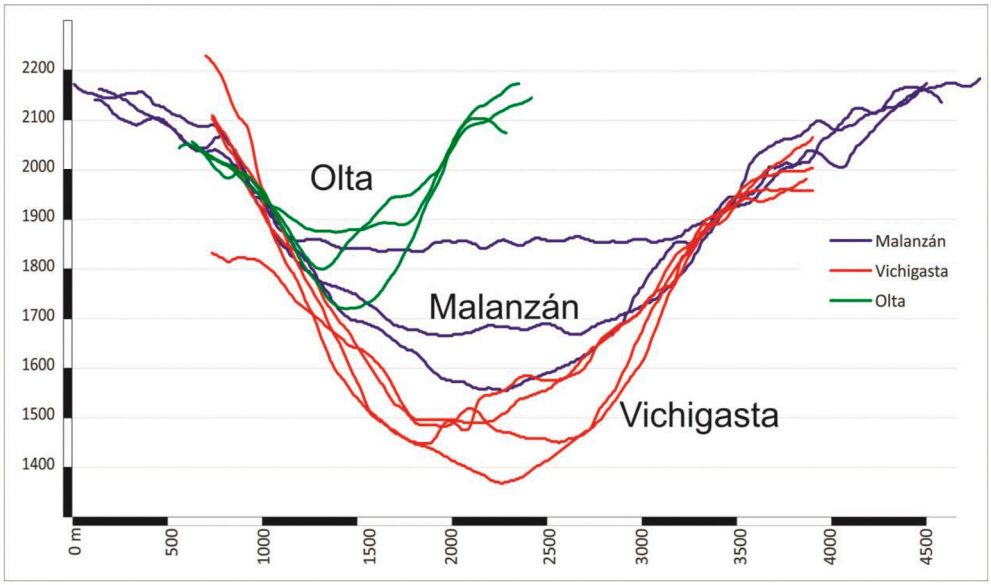

Fig. 7. Integrated profiles of the three paleovalleys. Notice the different size of each one. Olta could rank as a tributary valley compared to the other two.

suggesting Olta paleovalley may have been a minor tributary to Malanzán one (Fig. 7). The three transverse sections taken over the Malanzán paleovalley again suggest a U-shape, but are more affected than the Vichigasta by the elements that modify the original glacial profile. In the case of Malanzán paleovalley, the main problem is that the Carboniferous fill is irregularly still in place, a problem more acute on the westernmost (glacially downstream) profile, which as a result shows a very flat floor. In spite of the problem in the base of the paleovalley, there is a perfect match of the margins and shoulders of the Malanzán paleovalley, suggesting it was a conduit glacier of comparable size to Vichigasta. This paleovalley was slightly wider than Vichigasta as present-day profiles suggest c. 3 km width, but slightly shallower as the conduit would be full with a 600 m thick glacier. This produces an ice section of c. 3 km^2. On the other hand, Olta paleovalley width, as suggested by three transverse profiles along its course, indicates it was only c. 1 km wide and that only 300 m of ice would fill it up to the shoulders,

giving an ice section 0.33 km^2. Olta paleovalley is thus, one order of magnitude smaller in capacity than Malanzán. Hence, in order to add the needed ice to produce the latter, we checked the size of the Anzulón paleovalley (Pauls et al., 2019) that has been cited a potential tributary. Unfortunately, the terrain analysis did not work well at Anzulón paleovalley given the lack of a clean margin or shoulders elaborated on the basement. However, the Anzulón potential width is comparable to the Olta paleovalley, so we believe that perhaps other(s) tributaries added ice volume to the Malanzán collector as well. For instance, a tributary could run from north to south between the Malanzán and Los Llanos ranges (see Fig. 4 of Pauls et al., 2019). What becomes clear from the analysis of both Malanzán and Olta paleovalleys is that the width was roughly constant along stream, indicating that in all cases, they were transport valleys as suggested by modern measurements (Elvehoy et al., 1997) and mathematical models of glacial valley shapes (Anderson et al., 2006).

4.2.3. *Vichigasta paleodrumlin and erosional profiles*

An anomaly in the valley floor of Vichigasta paleovalley was also surveyed, which we interpret as a drumlin due to its higher slope pointing upstream (eastward), and gentle slope downstream (westward). Its position in the middle of the valley floor suggests a subglacial feature that could be interpreted as a drumlin. No fluvial process would generate such a feature in a very homogeneous basement such as in this part of the valley. Unfortunately, this feature is partially eroded and partially covered, and further study is required to confirm its origin.

Additional evidence that suggests glacial erosion is the profile found below the fan deltas of Stage 2 at the western part of the valley indicating an alternation of abrasion and plucking. As shown by Fig. 5 (D-E), the proposed glacier stoss side is smoothly dipping upstream whereas to the west, a step-wise profile is seen where boulders were extracted by plucking or quarrying, a process of glacial erosion on the lee sides of obstacles that characterizes the well-known *roches moutonnées*.

4.3. *Palynological assemblages: age and paleoenvironment significance*

All recovered palynomorphs were obtained from five productive samples in Stage 3 (Figs. 1D and 5B) that allowed the recognition of 61 species of terrestrial groups of plants and algae, which are represented by 48 trilete spores, 9 pollen grains and 4 fresh water algal species. Lycophytes (*Cristatisporites, Kraeuselisporites, Lundbladispora, Vallatisporites*), pteridophytes (e.g., *Anapiculatisporites*, *Convolutispora, Granulatisporites, Leiotriletes, Punctatisporites*) and monosaccate pollen grains of Cordaitean and Coniferalean are the most diverse groups (Figs. 8–11). The preservation of spores and phytoplankton is fairly-good with respect to pollen grains that exhibit a higher mechanical damage. Thermal

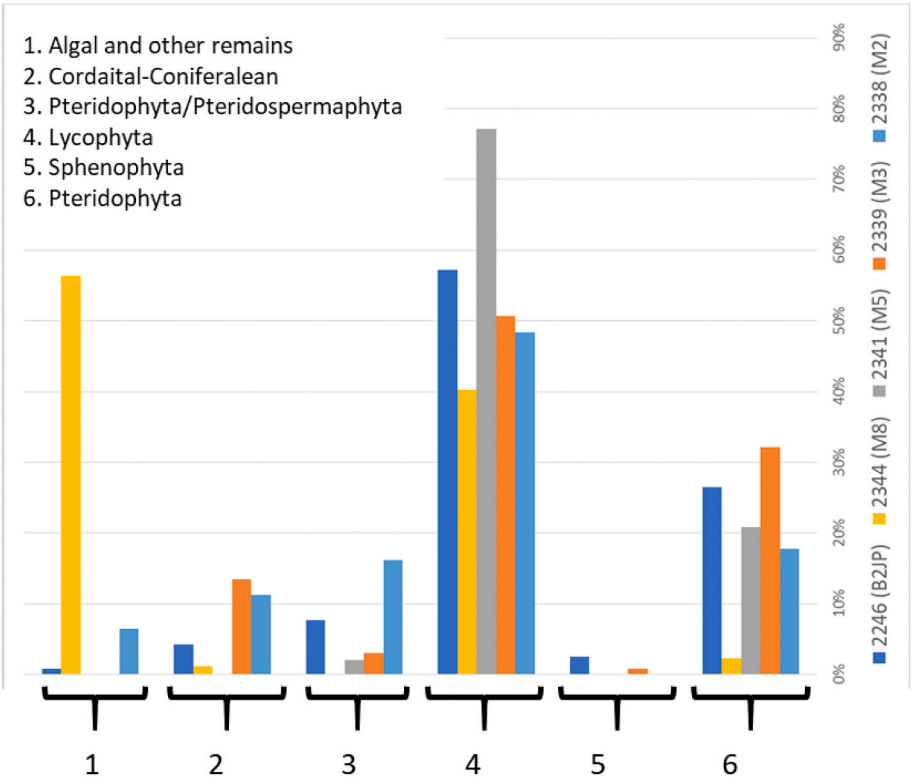

% Major paleobotanical groups of palynomorphs	2338 (M2)	2339 (M3)	2341 (M5)	2344 (M8)	2246 (B2)
Pteridophyta	18%	32%	21%	2%	26%
Sphenophyta	0%	1%	0%	0%	3%
Lycophyta	48%	51%	77%	40%	57%
Pteridophyta/ Pteridospermaphyta	16%	3%	2%	0%	8%
Cordaitalean-Coniferalean	11%	13%	0%	1%	4%
Algal and other remains	6%	0%	0%	56%	1%
Palynofacies= Phytoclasts/ Palynomorphs/ AOM	10% -90% -0%	1% -99% -0%	90% -10% -0%	50% -10% -40%	1% -99% -0%

Fig. 8. Percentage of major paleobotanical groups of palynomorphs and other palynofacies components per sample at Vichigasta.

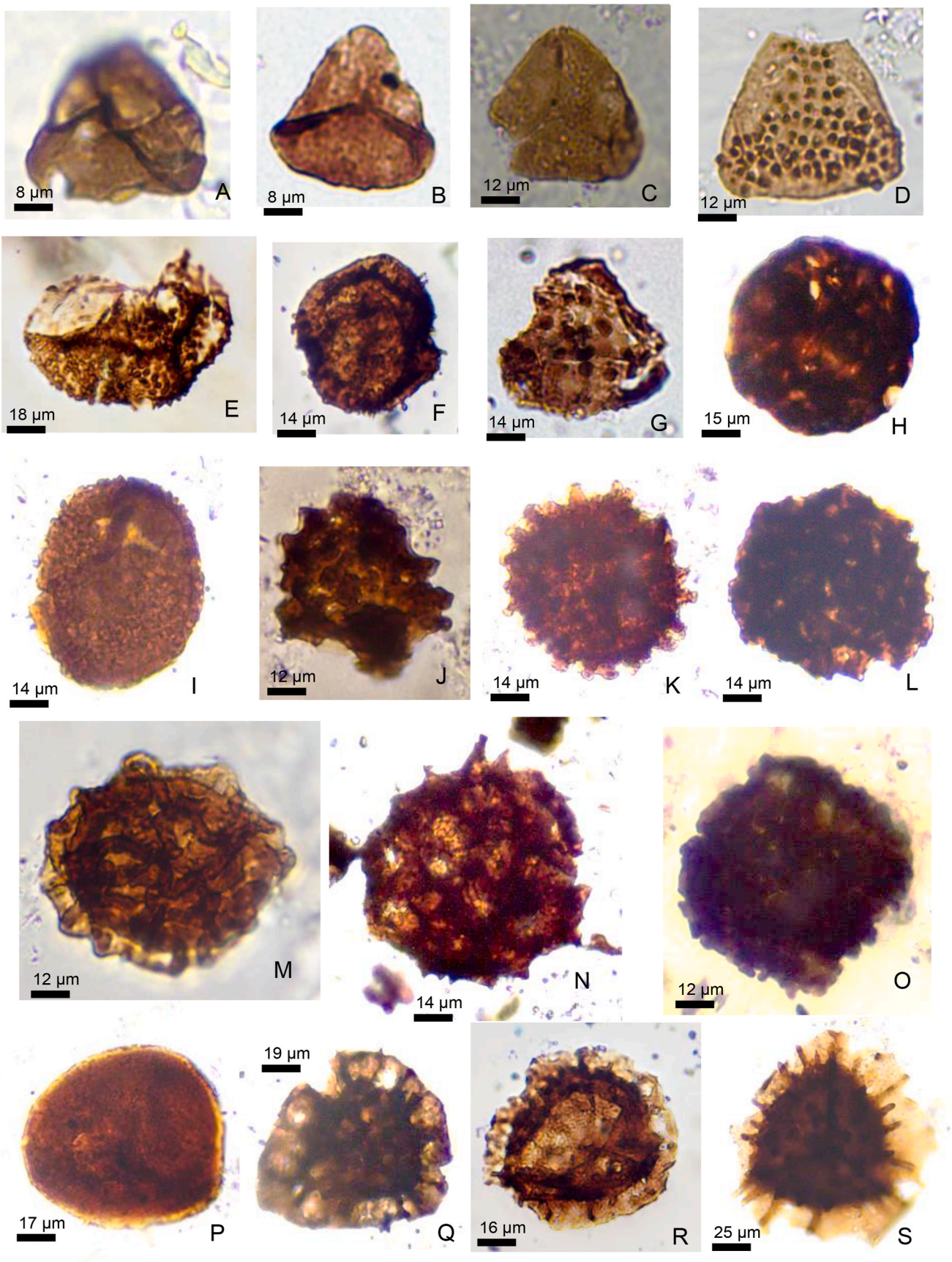

(caption on next page)

Fig. 9. A. Leiotriletes tumidus Butterworth & Williams, CICYTTP-Pl 2339 J25, B, C. *Granulatisporites austroamericanus* Archangelsky & Gamerro 1979, B. CICYTTP-Pl 2341 P31/4, C. CICYTTP-Pl 2346 D26, D. *Anapiculatisporites concinnus* Playford 1962, CICYTTP-Pl 2346 K21, E. *Dibolisporites disfacies* Jones & Truswell 1992, CICYTTP-Pl 2339 H30, F. *Apiculatisporis variornatus* di Pasquo, Azcuy & Souza 2003, CICYTTP-Pl 2341 V37/1, G. *Pustulatisporites papillosus* (Knox) Potonié & Kremp 1955, CICYTTP-Pl 2341 N31/4, H. *Foveosporites cf. pellucidus* Playford & Helby 1968, CICYTTP-Pl 2338 V38 .I. *Verrucosisporites patelliformis* (Menéndez) Limarino & Gutierrez 1990, CICYTTP-Pl 2346 T28, J. *Secarisporites irregularis* Azcuy 1975, CICYTTP-Pl 2346 N32/4, K. *Raistrickia rotunda* Azcuy 1975, CICYTTP-Pl 2346 X29/4, L. *Convolutispora muriornata* (Menéndez 1965), CICYTTP-Pl 2339 Q36/2, M. *Velamisporites cortaderensis* (Cesari & Limarino) Playford 2015, CICYTTP-Pl 2346 J46/1, N. *Reticulatisporites magnidictyus*, CICYTTP-Pl 2339 F43/4, O. *Cordylosporites asperdictyus* Playford & Helby 1968, CICYTTP-Pl 2339 F27/4, P. *Lundbladispora riobonitensis* Marques-Toigo & Picarelli, CICYTTP-Pl 2346 N52/1, Q. *Vallatisporites arcuatus* (Marques-Toigo) Archangelsky & Gamerro 1979, CICYTTP-Pl 2339 M28/2, R. *Kraeuselisporites volkheimerii* Azcuy 1975, CICYTTP-Pl 2341 S35/3, S. *Kraeuselisporites* sp., CICYTTP-Pl 2346 E31/2.

alteration index (TAI in Utting and Wielens, 1992) ranges between +2 and 3 (dark orange to brown). Quantitative and stratigraphic distribution of amorphous organic matter (AOM), phytoclasts (tracheids, cuticles, brown and black particles) and palynomorphs (palynofacies components) in the outcrop (Fig. 8) allows us to highlight general trends. Tracheids are most frequent in sample M5 followed by cuticles and brown and black particles whereas they are scarce in sample M2 and absent in the other two ones. Amorphous organic matter is only present in sample M8 in a similar frequency to phytoclasts. Concerning major groups of plants, lycophytes dominate in all samples (ca. 40–80%), followed by pteridophytes except in sample M8, in which *Botryococcus* is dominant (50%) together with the lycophyte *Lundbladispora* (40%). Among the pteridophytes, *Punctatisporites* is frequent (5–10%) to present (1–4%) in all the samples whereas *Cristatisporites* is the most abundant and diverse genus of lycophytes in almost all the samples except for M8. Of them, the most frequent species (>10%) are *Cristatisporites stellatus, C. menendezii, C. rollerii, C. inconstans* mainly documented in samples M5 and B2. In these two samples, *Granulatisporites austroamericanus* is well-represented, followed by *Kraeuselisporites volkheimerii* and *Cyclogranisporites australis* (mostly derived from pteridosperms). Cordaitean and Coniferalean are around 10–15% in the two lower samples M2 and M3. The sample M3 is the most diverse in spores and monosaccate pollen grains and several species of both groups are shared with M2 (e.g. *Anapiculatisporites concinnus, Cannanoropollis triangularis, Divarisaccus stringoplicatus, Potonieisporites neglectus, P. novicus*). It is noted the appearance of *Reticulatisporites magnidictyus* in sample M3 (see Fig. 12).

These assemblages are attributed to the late Serpukhovian-Bashkirian subzone A of the *Raistrickia densa-Convolutispora muriornata* (DM) Zone supported by the presence of monosaccate pollen grains and key spores *Convolutispora muriornata* and *Granulatisporites austroamericanus* and *Lundbladispora* with their FADs in the late Serpukhovian. Other well-represented species in our samples are *Velamisporites cortaderensis, C. menendezii* and *Cristatisporites stellatus,* known since the Visean mainly in southern South America, but they are widely documented in this Subzone.

The paleoenvironmental interpretation of each sample based on palynofacies features reveals changes across the dark shale deposit of Stage 3. It is noted that sample M8 is the most different in terms of preservation, diversity and frequency of species. Biodegraded *Lundbladispora* species (herbaceous lycophyte) and well–preserved chlorophycean *Botryococcus* are dominant, whereas monosaccate pollen grains are very scarce and *Cristatisporites* is absent. A very low frequency of the acritarch *Navifusa variabilis* is found in samples M8 and B2, which was also documented in the Malanzán Formation at the Olta Valley (Gutiérrez and Limarino, 2001), and farther to the west in the Veladero paleovalley (Limarino et al., 2014) (Fig. 1B). Limarino et al. (2014) support shallow brackish water environments occurred due to acritarchs are mostly of marine origin. The mixture of fresh water and brackish/shallow marine phytoplanktonic species in this paleovalley would reinforce a connection to the sea of eastern areas of Paganzo basin during the main DMa post-glacial transgressive event (Valdez et al., 2020 and references herein). The mentioned features in sample M8 (top of unit) together with the abundance of AOM mostly derived from phytoplankton (fluorescent) are evidence of an increase of the water level during the deposition of the Stage 3.

On the other hand, in samples M2, M3 and B2 predominate spore species of lycophytes and sphenophytes representing humid areas like in fluvial plains and protected areas of rivers and water bodies. Relatively close to these environments, arboreal stocks (forests) of Cordaitean and Coniferalean and pteridosperms were present in lower to higher more xerophytic landscapes. Pteridophytes are mostly part of both the understory in the forests and lowlands. The scarcity or absence of phytoclasts in samples M2, M3 and B2, which probably derived from the arboreal plants, could support their rapid settling when a relatively abrupt change of energy occurs during the transport, whereas lighter particles mostly palynomorphs and AOM were transported in suspension to be deposited farther in low energy protected areas of aquatic bodies.

5. Discussion

5.1. The glacial origin of Vichigasta paleovalley

Evidence presented in this contribution strongly supports a glacial origin for the Vichigasta paleovalley. Dropstones could result from seasonal freezing of the lake surface or even, they can be a product of vegetal rafting and used to discard a glacial origin of some dropstone-bearing sedimentary units (cf. Pauls et al., 2019). However, reported grain sizes associated with these processes in modern lakes never exceed 2–3 cm in diameter, and they are an exceptional process rather than a dominant one. Stage 1 deposits leave little room for doubt that it was glacier ice rafting that was responsible for emplacement of the outsize clasts, due to the excessive size of some drop-boulders (exceeding a couple of metric tons of weight), and for the potential dump structures described. Stage 1 also suggests the existence of minor ice re-advances during the general retreat that caused the horizontal faulting and meso-thrusting of small portions of the MTD and overlying turbidites and interbedded shales. We did not observe any fault extending from the basement to the Carboniferous fill, and to create these faults, an almost horizontal compressional force would have been needed. These observations suggest horizontal thrusting in Stage 1 could have been only created by glacio-tectonism, as it would be the only force acting horizontally within this unfaulted paleovalley. This compression direction matches the glacier flow direction indicated both by the erosional profile of the valley and by the subsequent outwash system (fluvial braided) of Stage 2, that developed after ice retreat. Stage 2 systems were probably responsible for eroding most glacio-related deposits of Stage 1. Additional but inconclusive evidence of the glacial flow is the morphology of the basement mound in the middle of the valley, whose best interpretation is of a drumlin remnant.

On top of the sedimentological and stratigraphic evidence, the unavoidable fact is that this paleovalley shows a classical U-shape. As shown in the terrain analysis section, this is not the only Carboniferous paleovalley showing this shape. The comparison between this and others elaborated over the same type of bedrock (crystalline basement), using DEM analysis, indicates a shared origin of these valleys.

Another element to judge on the origin of the paleovalley is its regular shape downstream. We do not know of any fluvial valley that maintains such uniform width downstream, whereas glacial valleys, particularly those significantly long, tend to acquire a constant width until the first 20% of its length is passed by, as suggested by models based on real data of modern glaciers (Elvehoy et al., 1997; Anderson et al., 2006). Thus, the regularity of width and shape in the flow

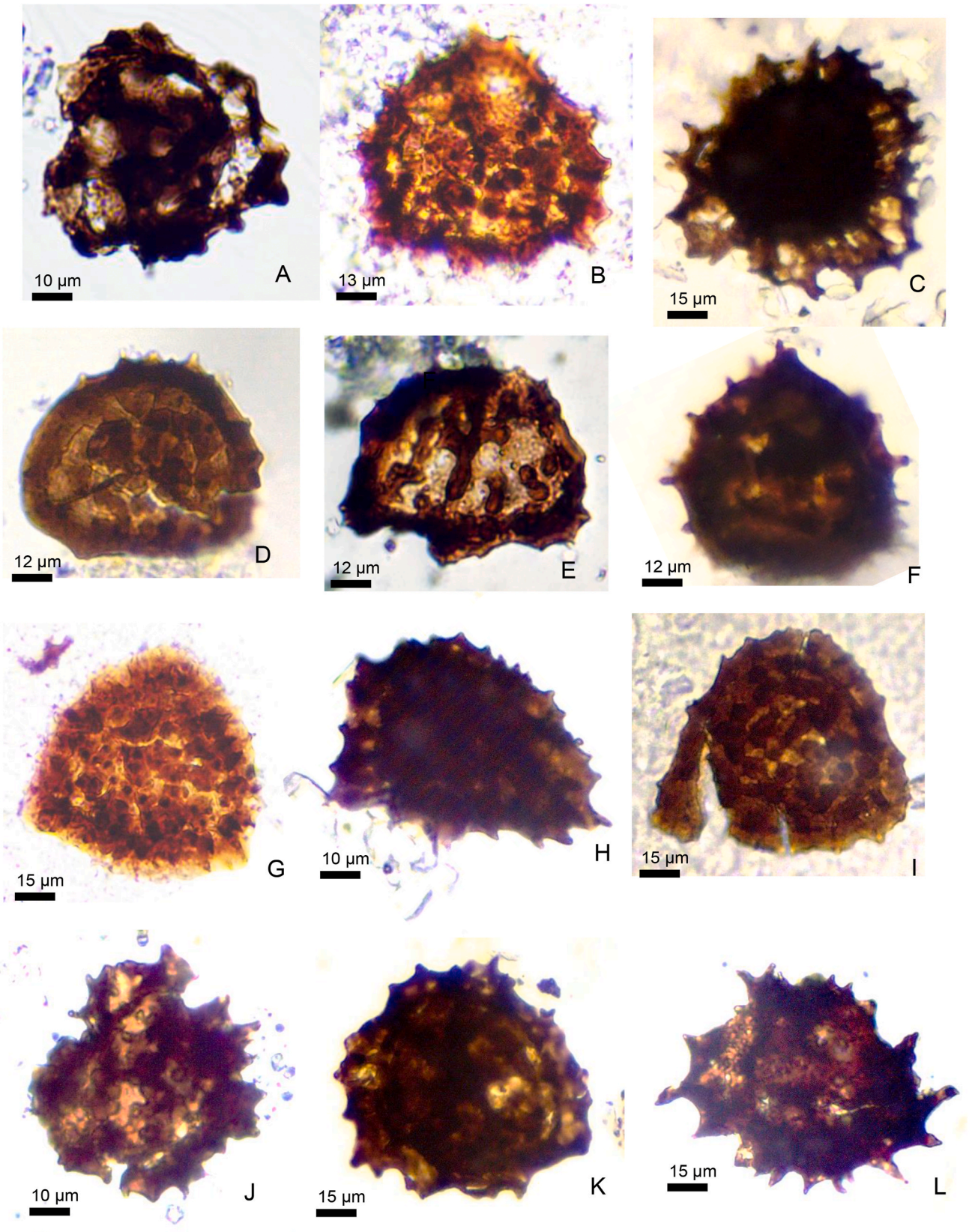

Fig. 10. A, B. Cristatisporites inordinatus (Menéndez & Azcuy) Playford 1978, CICYTTP-Pl 2339 B63, CICYTTP-Pl 2346 W62/3, C. Cristatisporites chacoparanaensis Ottone 1989, CICYTTP-Pl 2338 G60. D-F. Cristatisporites stellatus (Azcuy) Limarino & Gutierrez 1990, D. CICYTTP-Pl 2346 O56/1, E. CICYTTP-Pl 2341 X24/3, F. CICYTTP-Pl 2338 X25/4, G, I. Cristatisporites menendezii (Menéndez & Azcuy) Playford emend. Césari (1985), G. CICYTTP-Pl 2346 Z62/1, I. CICYTTP-Pl 2346 M31, H. Cristatisporites scabiosus Menéndez 1965, CICYTTP-Pl 2338 Q24/2, J. Cristatisporites inconstans Archangelsky & Gamerro 1979, CICYTTP-Pl 2339 F43/3, K. Cristatisporites rollerii Ottone 1998, CICYTTP-Pl 2338 H23. L. Spinozonotriletes hirsutus Azcuy 1975, CICYTTP-Pl 2339 E45/3.

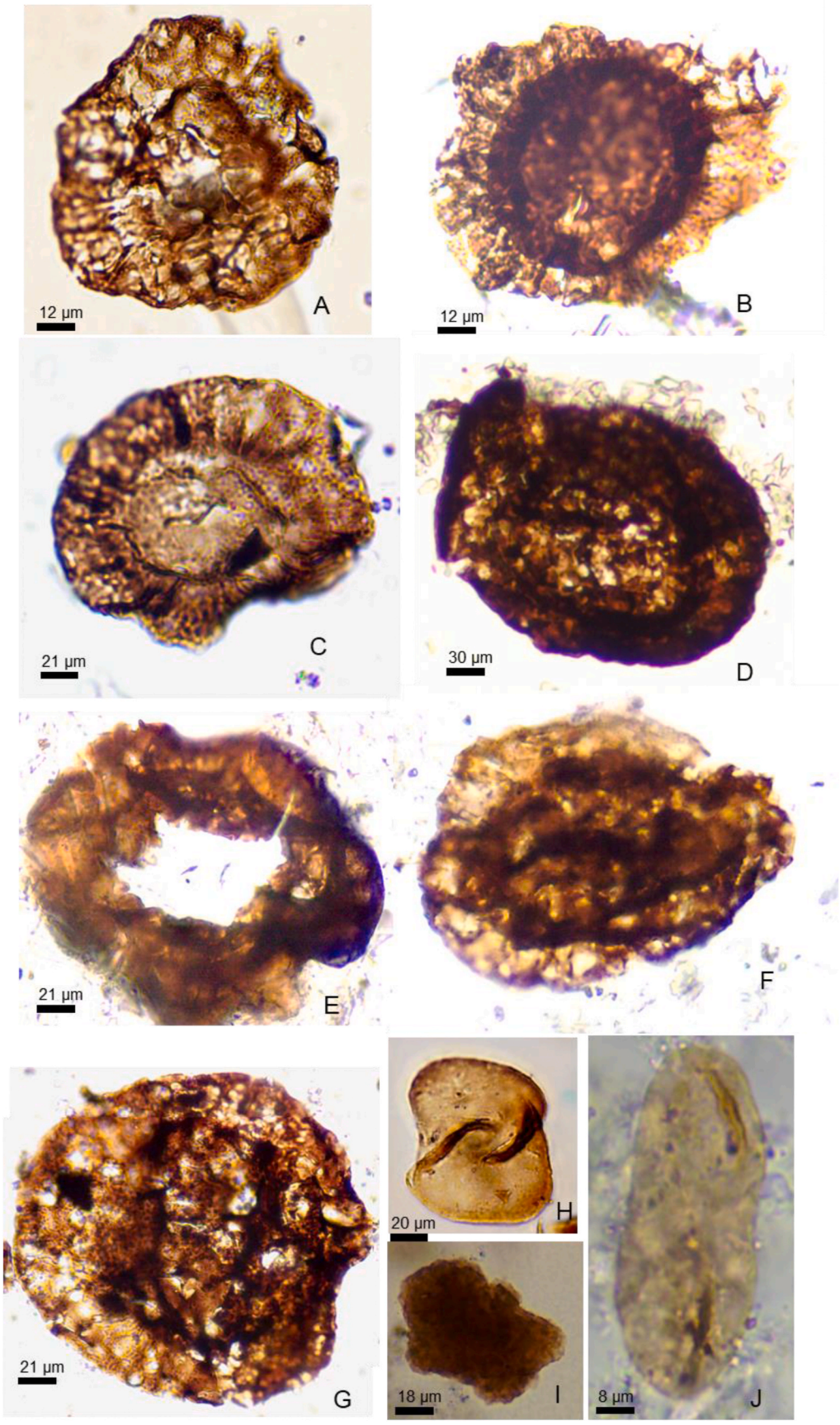

Fig. 11. A. *Cannanoropollis triangularis* (Mehta) Bose & Maheshwari 1968, CICYTTP-Pl 2339 P29/4, B. *Plicatipollenites malabarensis* (Potonié & Sah) Foster 1975, CICYTTP-Pl 2339 B33/4, C. *Cannanoropollis janakii* Potonié & Sah 1960, CICYTTP-Pl 2339 O31, D. *Potonieisporites novicus* Bharadwaj 1954, CICYTTP-Pl 2338 M55/3, E. *Potonieisporites neglectus* Potonié & Lele 1961, CICYTTP-Pl 2339 Z36/2, F. *Divarisaccus stringoplicatus* Ottone 1991, CICYTTP-Pl 2339 W40/3, G. *Potonieisporites magnus* Lele & Karim 1971, CICYTTP-Pl 2339 D24/4, H. *Tetraporina punctata* (Tiwari & Navale) Kar & Bose 1976, CICYTTP-Pl 2344 H44, I. *Botryococcus braunii* Kützing, CICYTTP-Pl 2344 M57, j. *Navifusa variabilis* Gutierrez & Limarino 2001, CICYTTP-Pl 2346 X31.

Species / CICYTTP-PI	2338 (M2)	2339 (M3)	2341 (M5)	2344 (M8)	2246 (B2JP)	AF. BOT.	Global range
Anapiculatisporites concinnus Playford 1962	2%	3%			3%	P	Visean-Pennsylv
Convolutispora spp.	2%	4%				P	
Foveosporites cf. *pellucidus* Playford & Helby 1968	3%					P	Vis-Bashkirian
Leiotriletes spp. (mostly *L. tumidus* Butterworth & Williams 1958)	3%	10%			3%	P	
Punctatisporites spp. (*P. pseudofoveosus* Azcuy 1975 and others	5%	4%	10%	2%	6%	P	
Pustulatisporites spp.	2%	1%				P	
Raistrickia radiosa? Playford & Helby 1968	2%	1%				P	Visean-Pennsylv
Cristatisporites chacoparanaensis Ottone 1989	2%				1%	L	la Serp-Permian
Cristatisporites inconstans Archangelsky & Gamerro 1979	5%	6%	2%		2%	L	Visean-Permian
Cristatisporites menendezii (Menéndez & Azcuy) Playford emend. Césari 1976	5%	2%	13%		10%	L	Visean-Permian
Cristatisporites rollerii Ottone 1998	5%	5%	2%		7%	L	Visean-Pennsylv
Cristatisporites scabiosus Menéndez 1965	8%	4%	2%		5%	L	Visean-Permian
Cristatisporites stellatus (Azcuy) Limarino & Gutiérrez 1990	5%	10%	15%		9%	L	Vis-Bashkirian
Cristatisporites spp.	16%	15%	31%		13%	L	
Lundbladispora riobonitensis Marques Toigo & Picarelli 1985	3%			11%	2%	L	la Serp-Permian
Cannanoropollis triangularis (Mehta) Bose & Maheshwari 1968	2%	2%			1%	C-C	la Serp-Permian
Divarisaccus stringoplicatus Ottone 1991	2%	1%				C-C	la Serp-Permian
Potonieisporites neglectus Potonié & Lele 1961	2%	1%				C-C	la Serp-Permian
Potonieisporites novicus Bharadwaj 1954	2%	1%				C-C	la Serp-Permian
Botryococcus braunii Kützing	6%			46%		A	late Devonian-Present
Apiculatasporites caperatus Menéndez & Azcuy 1969		1%			2%	P	Visean-Pennsylv
Convolutispora muriornata Menéndez 1965		1%			1%	P	la Serp-Pennsylv
Convolutispora sculptilis Felix & Burbridge 1967		1%				P	la Serp-Pennsylv
Dibolisporites disfacies Jones & Truswell 1992		1%				P	Vis-Pennsylvanian
Pustulatisporites papillosus (Knox) Potonié & Kremp 1955		1%	2%			P	Vis-Pennsylvanian
Reticulatisporites magnidictyus Playford & Helby 1968 (= *R. riverosii* Ottone 1991 in P. Loinaze 2009)		1%				P	la Vis-Bashkirian
Cordylosporites asperdictyus (Playford & Helby 1968) Dino & Playford 2002		1%				P	Vis-Bashkirian
Retusotriletes sp.		2%				P	
Waltzispora polita (Hoffmeister, Staplin & Malloy) Smith & Butterworth 1967		1%				P	Vis-Pennsylvanian
Calamospora spp.		1%			2%	S	
Cristatisporites inordinatus (Menéndez & Azcuy) Playford 1978		1%			3%	L	Vis-Pennsylvanian
Cristatisporites spinosus (Menéndez & Azcuy) Playford emend. Césari 1986		1%			2%	L	Vis-Pennsylvanian
Densosporites annulatus (Loose) Smith & Butterworth 1967		2%	4%			L	a Devonian-Pennsylvania
Spinozonotriletes hirsutus Azcuy 1975		1%	2%			L	Vis-Pennsylvanian
Vallatisporites arcuatus (Marques-Toigo) Archangelsky & Gamerro 1979		2%			1%	L	Vis-Pennsylvanian
Cannanoropollis janakii Potonié & Sah 1960		1%				C-C	la Serp-Permian
Plicatipollenites malabarensis (Potonié & Sah) Foster 1975		1%				C-C	la Serp-Permian
Potonieisporites magnus Lele & Karim 1971		1%				C-C	la Serp-Permian
Potonieisporites spp.		3%				C-C	la Serp-Permian
Convolutispora ordonensis Archangelsky & Gamerro 1979			2%			P	la Serp-Permian
Granulatisporites austroamericanus Archangelsky & Gamerro 1979			4%		9%	P	la Serp-Permian
Kraeuselisporites volkheimerii Azcuy 1975			4%		1%	L	la Vis-Permian
Kraeuselisporites sp.			2%			L	
Cyclogranisporites australis Azcuy 1975			2%		1%	Pt	la Serp-Permian
Apiculatisporis variornatus di Pasquo, Azcuy & Souza 2003			2%			P	Vis-Pennsylvanian
Lundbladispora braziliensis (Pant & Srivastava) Marques-Toigo & Pons 1986				29%	1%	L	la Serp-Permian
Circumplicatipollis plicatus Ottone & Azcuy 1988				1%		C-C	la Serp-Permian
Brazilea scissa (Balme & Hennelly) Foster 1975				3%		A	Late Paleozoic
Navifusa variabilis Gutierrez & Limarino 2001				1%	1%	A	la Serp-Pennsylv
Tetraporina punctata (Tiwari & Navale) Kar & Bose 1976				6%		A	Late Paleozoic
Raistrickia rotunda Azcuy 1975 (=? *R. accinta* in Playford 2015)					1%	A	la Vis-Pennsylvanian
Retusotriletes anfractus Menéndez & Azcuy 1969					1%	A	la Serp-Pennsylv
Secarisporites irregularis Azcuy 1975					1%	A	la Serp-Pennsylv
Verrucosisporites patelliformis (Menéndez) Limarino & Gutiérrez 1990					1%	A	la Serp-Pennsylv
Verrucosisporites sp.					1%	A	
Calamospora hartungiana Schopf in Schopf, Wilson & Bentall 1944					1%	S	la Serp-Permian
Velamisporites cortaderensis (Cesari & Limarino) Playford 2015					2%	L	la Vis-Pennsylvanian
Stenozonotriletes sp.					1%	L	
Cyclogranisporites firmus Jones & Truswell 1992					1%	Pt	Vis-Pennsylvanian
Cyclogranisporites spp. (*C. lasius*, others)					3%	Pt	
Kraeuselisporites malanzanensis Azcuy 1975					1%	L	la Serp-Pennsylv
Spores (poorly preserved)	16%	3%			3%		
Monosaccate pollen (poorly preserved)	5%	4%			3%	C-C	la Serp-Triassic
Pteridophyta (P)	18%	32%	21%	2%	26%		
Sphenophyta (S)	0%	1%	0%	0%	3%		
Lycophyta (L)	48%	51%	77%	40%	57%		
Pteridophyta/Pteridospermaphyta (Pt)	16%	3%	2%	0%	8%		
Cordaitean-Coniferalean (C-C)	11%	13%	0%	1%	4%		
Phytoplankton (A)	6%	0%	0%	56%	1%		
	10%	1%	90%	50%			
	90%	99%	10%	10%	1% 99%		
Palynofacies= Phytoclasts/ Palynomorphs/ AOM	0%	0%	0%	40%	0%		

Fig. 12. Stratigraphic distribution of the species documented at Vichigasta. For selected literature to support global range of species, see Milana and Di Pasquo et al. (2019) and Valdez et al. (2020) and their references. Botanical affinities: Pteridophyta (P), Sphenophyta (S), Lycophyta (L), Pteridophyta/Pteridospermaphyta (Pt), Cordaitean-Coniferalean (C–C), Phytoplankton (A).

direction, besides reaffirming it had a glacial origin, also indicates the glacier was not a mountain or alpine glacier, but a bypass glacier. Thus, the terrain analysis helped to argue that the Vichigasta paleovalley was carved by a bypass or outlet glacier, which matches perfectly with the general lack of glacigenic deposits as the glacier was, at the study area, transporting ice and sediment, and not having any depositional function.

5.2. The glaciation type and its paleogeographic implication

The size and regularity of this paleovalley suggest a conduit glacier. This implies that the Vichigasta glacier was transporting large amounts of ice towards the west. There is no evidence of any glacial transport from west to east, neither stratigraphic nor compositional. All known glacial and proglacial deposits in the Precordillera contain pebbles, cobbles and boulders from a crystalline basement (Kneller et al., 2004; Valdez et al., 2017), and they are documented only to the eastern region. None of the glacial systems in localities to the east of the Precordillera contains rock fragments sourced from the Precordillera. The evidence from sediment provenance that glaciers were moving sediment generically from east to west is thus incontrovertible, a logical process given the fact marine-dominated sequences for that stratigraphic period were located to the west. Therefore, we suggest that around the mid-Carboniferous, a network of outlet glaciers was moving ice and sediments for hundreds of km towards the west. In the case of the Vichigasta paleovalley, we believe that part of the material evacuated ended in deposits of the Cerro Bola depocenter, but also some glaciers reached what is now the boundary between the Precordillera and Cordillera, producing striated pavements (López-Gamundí and Martinez, 2000), and remains of glacial paleovalleys near that boundary (Milana and Di Pasquo, 2019).

There is no doubt that the Pampean ranges were not a typical craton, but probably a group of terranes accreted to the main South America continental mass (cf. Ramos et al., 1986; Steenken et al., 2004). Hence, there was some mobility along sutures, with occasional basin-forming processes occurring subsequently. All basement blocks belonging to what is now a broken foreland geological province, known as Sierras Pampeanas, share a similar aspect: they all have a flat top, slightly tilted during the Neogene orogeny. The timing when this peneplain developed and when the basement was slightly positively exposed is Triassic according to Jordan et al. (1989), using thermo-chronometric techniques. They found a significant correlation between the closure temperatures of minerals using fission track dating. Here lies the importance of Malanzán paleovalley: thermo-chronometric studies applied specifically to this paleovalley show different closure temperatures of the basement between the bottom of the paleovalley and its margins, suggesting there was up to 2 km of relief between valley floor and margins (Enkelmann et al., 2014) within a single basement block. This interpretation actually diminishes the potential size of outlet glaciers, as we interpreted the original valley shoulder when valley sides merged with the peneplain that was, according to Jordan et al. (1989) elaborated c. 100 Ma later. Thus, the peneplain that we use in this paper to model de valley shoulder would not represent the upper part of the Carboniferous paleovalley as the upper part was a product elaborated afterwards. The type of erosion of the peneplain development was not associated with a tectonic block or large uplifts, but with a generally uplifted area as plateaus are. Therefore, our vision of the paleovalleys might be just the lower part of these valleys and not the complete version of the original glacial paleovalley.

In this area of the Paganzo basin (Pampean ranges), there is no known orogenic process that could be responsible for this anomaly in mineral closure temperatures, so the most likely interpretation is that glaciers were carving valleys up to 2 km deep within the continental interior. Thus, the Malanzán section is very important reconstructing the glacial paleogeography as it lies at c. 300 km in a straight line from the 'open marine' paleovalleys of Hoyada Verde. If we consider the c. 80% shortening of the Precordillera fold and thrust belt (Allmendinger et al., 1990) and the c. 20% of shortening of the Sierras Pampeanas broken foreland, the original distance between Hoyada Verde and Malanzán would be 400–500 km. Thus, we insist on the existence of a large ice-sheet of the magnitude of the North American or North European that probably maintained a network of glaciers of that extent.

We cannot know the exact extent of the mid-Carboniferous ice-sheet that fed these outlet glaciers, but we suggest there is no other way to explain the sum of the evidence without a large ice-sheet located eastwards. We suggest this ice sheet was feeding the glacial and proglacial system of Paganzo basin to the west, and possibly other systems to the north and east.

5.3. The postglacial eustatic rise

An important fact to consider is the magnitude of the Bashkirian postglacial transgression in the Paganzo basin. While it is difficult to assure that Stage 3 mudstones have a marine component, it is also difficult to explain why all lower Bashkirian successions show the same scheme of flooding almost all over the Paganzo basin realm (cf. Valdez et al., 2020). It is difficult to explain such impressive synchronicity of flooding over a large area without falling into a eustatic explanation. Here comes the last evidence of the type of glaciers: alpine valley glaciers may show some characteristics of outlet glaciers as the basic U-shape described in this work. Although they differ in the general gradient of the valley. The alpine glaciers are polythermal because they start high, in a cold based and descend fairly-rapid to turn into a wet based, and well-lubricated glacier. On the other hand, outlet glacier valleys tend to be all the way wet-based, and hence they could keep low gradients for hundreds of kilometers.

Flooded valleys in the Norwegian coast let the sea to enter more than a hundred kilometers into the continent, in a glacial system that today could be partially comparable to an alpine type one, but the valleys were carved when the glaciation was the type of ice-sheet, and glacier valleys were formed on today's submerged shelf edge adding several kilometres more. However, what would happens if we consider some sectors with preferential subsidence as the Baltic, in the Norwegian scheme? In that case the sea could enter thousands of kilometres along wide areas and then along moderate valleys as the Vichigasta one. In such scenario, our Baltic sea undoubtedly is the Cerro Bola depocenter (Valdez et al., 2020) that, instead of being wiped out by the mid-Carboniferous glacial advance, received all the sediment transported in a true depositional area. Thus, the fact we can find postglacial transgressive muds so far inside the craton also suggests low-gradient valley glaciers that are not compatible with any alpine-type glaciation (Fallgatter et al., 2019; Valdez et al., 2017, 2020).

Other evidence suggesting the ice-sheet glacial model is the scarcity of primary glacial deposits. This argument was already used by Milana and BercowskI (1987) to propose a glacial model in the Precordillera where primary glacial deposits are present but scarce. In the Vichigasta area, which ranks as more 'interior', the absence of primary glacial deposits is expected due to the fact an ice sheet cannot produce much sediment (cf. Eyles et al., 1995). Most of the sediment, mainly carved from the floor and valley margins is taken by the glacier and transported towards depositional centers, which in this case could correspond to areas of Cerro Bola sub-basin where the entire glacial episode was preserved (Valdez et al., 2020).

6. Conclusions

Vichigasta paleovalley is a key locality for understanding the glacial context of LPIA in western Gondwana given the high level of preservation of paleo-geomorphological features. On top of the geomorphological evidence, the erosive remnants left within this paleovalley add important information for the complete understanding of this and some other glacial localities. All the available evidence indicates a glacial origin for the valley, also suggesting that it was an outlet glacier draining

a large ice sheet located to the east.

Evidence supporting the glacial origin is: (a) large ice-rafted boulders of Stage 1, (b) U-valley shape; (c) similarity of this valley shape with that at Malanzán; (d) regularity of valley shape and width downstream; (e) subglacial erosion profile of abrasion/plucking; (f) potential drumlin.

An outlet glacier interpretation is supported by: (a) size of the Vichigasta and Malanzán valleys suggests a maximum conduit section of c. 3 km^2 of ice and Olta is only a tributary with a bankfull section of 0.33 km^2 of ice; (b) regular U-shape downstream suggesting they are 'ice-transporting' valleys; (c) low-gradient of Vichigasta and similar paleo-valleys (Malanzán, Las Lajas, Quebrada Grande) allow deposition of the same transgressive shales as proven by identical palyno-age; (d) absence of any primary glacial deposits within this 'inner' sequence.

Therefore, we conclude that the mid-Carboniferous glaciation was not associated with any west-lying mountain range or a humidity gradient from west to east, and it was not a localized phenomenon, but a continental glaciation comparable to the Pleistocene North American or Scandinavian ice sheets at their maximum. Several evidences support the interpretation of an ice-sheet at the eastern Paganzo basin: a) distribution of moderate-size glacial paleovalleys at low areas, b) marine flooding of many of those paleovalleys, c) lack of thick and immature glacial sequences, d) transport of very coarse sediments for long distances (e.g. an erratic boulder of c. 5 m has been described very up on the sequence of Quebrada Grande at Precordillera), e) provenance of exotic clasts in proglacial beds from the Pampean ranges, f) absence of any type of alpine-glacier sedimentary succession. g) distance of marine fossil deposits from the expected coastal sequences (c. 100 km considering shortening), h) total distance of the mid-carboniferous post-glacial marine as expected. On the other hand, there is no evidence of alpine glaciation or an evident paleo-mountain and their associated side-basins. Future studies should focus on understanding better the location of the bypass areas and the depositional ones, as we believe it is not correct to name a collection of paleovalley fills as a sedimentary basin.

Author statement

I attest that all authors contributed to the elaboration of this manuscript. Dr. Victoria Valdez Buso and Dr. Juan Pablo Milana mapped, and worked in the sedimentary record of the valley. Dr. Mercedes di Pasquo sampled and analyzed the palinologic content. Mr. José Espinoza Aburto build up the DEMs.

Declaration of competing interest

The authors declare that they have no known competing financial interests or personal relationships that could have appeared to influence the work reported in this paper.

Acknowledgements

The authors thanks to Lic. Leonardo Silvestri for his help in sample processing at the CICYTTP (CONICET-ER-UADER) and *Consejo Nacional de Investigaciones Científicas y Técnicas* CONICET PIP 0812 (2015–2017). We thank Dr. Ben Kneller for his critical observations. We are also grateful to an anonymous reviewer and Dr. Claus Fallgatter for their comments that helped improved our work.

Appendix A. Supplementary data

Supplementary data to this article can be found online at https://doi.org/10.1016/j.jsames.2020.103066.

References

Allmendinger, R.W., Figueroa, D., Snyder, D., Beer, J.C., 1990. Mpodozis., B. L. Isacks. 1990. Foreland shortening and crustal balancing in the Andes at 30^0 latitude. Tectonics 9 (4), 789–809.

Andreis, R.R., Archangelsky, S., Leguizamón, R.R., 1986. El paleovalle de Malanzán: nuevos criterios para la estratigrafía del Neopaleozoico de la sierra de Los Llanos, La Rioja, República Argentina, vol. 57. Boletín de la Academia Nacional de Ciencias (Córdoba), pp. 1–119.

Anderson, R.S., Molnar, P., Kessler, A.M., 2006. Features of glacial valley profiles simply explained. J. Geophys. Res. 111, F01004. https://doi.org/10.1029/2005JF000344.

Astini, R.A., Martina, F., Ezpeleta, M., Dávila, F.D., Cawood, P.A., 2009. Chronology from Rifting to Foreland Basin in the Paganzo Basin (Argentina), and a Reapprisal on the "eo- and Neohercynian" Tectonics along Western Gondwana., XII Congreso Geológico Chileno, Santiago, Chile. Universidad de Chile, Santiago, Chile, pp. 1–4. Extended Abstracts S9 010.

Archangelsky, S., Gamerro, J.C., 1979. Palinología del Paleozoico superior en el subsuelo de la Cuenca Chacoparanense, República Argentina. I. Estudio sistemático de los palinomorfos de tres perforaciones de la provincia de Córdoba. Revista Española de Micropaleontología 11 (3), 417–478.

Astini, R., 2010. Linked basins and sedimentary products across an accretionary margin: the case for the late history of the peri-Gondwanan Terra Australis orogen through the stratigraphic record of the Paganzo Basin. In: Papa, C., Astini, R. (Eds.), Field Excursion Guidebook, 18th International Sedimentological Congress. International Association of Sedimentologists, Mendoza, Argentina, p. 58.

Amos, A.J., Rolleri, E.O., 1965. El Carbonico marino en el Valle Calingasta-Uspallata (San Juan-Mendoza). Bol.Inf. Petroleras, Buenos Aires, pp. 1–23.

Aquino, C.D., Milana, J.P., Faccini, U.F., 2014. New glacial evidences at the Talacasto paleofjord (Paganzo basin, W-Argentina) and its implications for the paleogeography of the Gondwana margin. J. South Am. Earth Sci. https://doi.org/10.1016/j.jsames.2014.09.001.

Augustunuz, P.C., 1995. Glacial valley cross-profile development: the influence of in situ rock stress and rock mass strength, with examples from the Southern Alps, New Zealand. Geomorpholigy 14, 87–97.

Azcuy, C. y Morelli J., 1970. Geología de la comarca Paganzo-Amaná. El Grupo Paganzo. Formaciones que lo componen y sus relaciones. Rev. Asoc. Geol. Argent. 25, 405–429.

Azcuy, C.L., 1975. Miosporas del Namuriano y Westfaliano de la Comarca Malazán-Loma Larga, Província de La Rioja, Argentina. II. Descripciones sistemáticas y significado estratigráfico de las microfloras. Ameghiniana 122, 113–163.

Azcuy, C.L., Andreis, R., Cuerda, A., Hünicken, M., Pensa, M., Valencio, D.A. y, Vilas, J. F., 1987. III cuenca Paganzo. In: Archangelsky, S. (Ed.), El Sistema Carbonífero en la República Argentina. Academia Nacional de Ciencias, Córdoba, pp. 41–99.

Azcuy, C.L., Carrizo, H.A., Caminos, R., 2000. Capítulo 12, Carbonífero y Pérmico de las Sierras Pampeanas, Famatina, Precordillera, Cordillera Frontal y Bloque San Rafael. Geología Argentina: in: Caminos, R. (Ed.). Anales Instituto de Geología y Recursos Minerales 26 (11), 261–317.

Batten, D.J., 1996. Palynofacies. 26B-palynofacies and petroleum potential. In: Jansonius, J., McGregor, D.C. (Eds.), Palynology: Principles and Applications, vol. 3. American Association Stratigraphic and Palynologists Foundation, pp. 1065–1084.

Bharadwaj, D.C., 1954. Einige neue Sporengattungen des Saarkarbons. Neues Jahrb. Geol. Paläontol. Monatsh 11, 512–525.

Bose, M.N., Maheshwari, H.K., 1968. Palaezoic *Sporae dispersae* from Congo. VII - Coal measures near lake Tanganyika, South of Albertiville. Ann. Mus. R. Af. Cent., Sc. Geol., Ser. 8 60, 116.

César, S.N., 1985. Palinología de la Formación Tupe (Paleozoico superior), Sierra de Maz, provincia de La Rioja. Parte II. Ameghiniana 22, 107–212.

César, S.N., Gutierrez, P., Sabattini, N., Archangelsky, A., Azcuy, C.L., Carrizo, H.A., Cisterna, G., Crisafulli, A., Cúneo, R.N., Díaz Saravia, P., Di Pasquo, M.R., González, C.R., Lech, R., Pagani, M.A., Sterren, A., Taboada, A.C., Vergel, M.M., 2007. Paleozoico Superior de Argentina: un registro fosilífero integral para el Gondwana Occidental. Publicacion Espec. - Asoc. Paleontol. Argent. 11, 35–54.

Di Paola, E., 1972. Caracterización litoestratigráfica de la Formación Lagares (Carbónico), en Paganzo-Amaná, provincia de La Rioja, República Argentina. Rev. Asoc. Geol. Argent. 27, 99–116.

di Pasquo, M.M., Silvestri, L., 2014. Las colecciones de palinología y paleobotanica del laboratorio de paleopalinología y paleobot anica del centro de investigaciones científicas y transferencia de tecnología a la produccion (CICYTTP), Entre Ríos, Argentina. Contrib. _a RESCEPP "Rede Sul-americana Coleç~oes Ensino em Paleobotânica Palinologia". Bol. Asoc. Latinoam. Paleobotanica Palinol. 14, 39–47.

Di Pasquo, M., Azcuy, C.L., Souza, P.A., 2003. Palinología del Carbonífero Superior del Subgrupo Itararé en Itaporanga, Cuenca Paraná, Estado de São Paulo, Brasil. Parte 2: sistemática de polen y significado paleoambiental y estratigráfico In Ameghiniana, pp. 297–313 no. 3, 40.

Di Pasquo, M.M., Folnagy, H.J.A., Isaacson, P.E., Grader, G.W., 2019. Late paleozoic carbonates and glacial deposits in Bolivia and northern Argentina: significant paleoclimatic changes. SEPM (Soc. Sediment. Geol.) Spec. Publ. 108, 185–203. https://doi.org/10.2110/sepmsp.108.10.

Enkelmann, E., Ridgway, K.D., Carignano, C., Linnemann, U., 2014. A Thermochronometric View into an Ancient Landscape: Tectonic Setting, and Inversion of the Paleozoic Eastern Paganzo Basin, Argentina. Lithosphere, vol. 6, pp. 93–107.

Elvehoy, H., Haakensen, N., Kennett, M., Kjollmoen, B., Kohler, J., Tvede, A.M., 1997. Glasiologiske Undersokelser I Norge 1994 Og 1995, Publ. 19. Norges Vassdrags og Energiverk, Oslo.

Eyles, N., Gonzales Bonorino, G., França, A.B., Eyles, C.H., 1995. Hydrocarbon-bearing late Palaeozoic glaciated basins of southern and central South America. In: Tankard, A.J., Suárez-Soruco, R., Welsink, H.J. (Eds.), *Petrol. Basins S. Am.* Am. Assoc. Pet. Geol. Memoir, vol. 62, pp. 165–183.

Eyles, N., 1993. Earth's glacial record and its tectonic setting. Earth Sci. Rev. https://doi.org/10.1016/0012-8252(93)90002-O.

Fallgatter, C., Valdez Buso, V., Paim, P.S.G., Milana, J.P., 2019. Stratigraphy and depositional architecture of lobe complexes across a range of confinements: examples from the late Paleozoic Paganzo Basin, Argentina. Mar. Petrol. Geol. 110, 254–274, 1223.10.1016/j.marpetgeo.2019.07.020.

Fielding, C.R., Frank, T.D., Isbell, J.L., 2008. The late Paleozoic ice age - a review of current understanding and synthesis of global climate patterns. Spec. Pap. Geol. Soc. Am. https://doi.org/10.1130/2008.2441(24.

Foster, C.B., 1975. Permian plant microfossils from the Blair Athol Coal Measures, Central Queensland, Australia. Palaeontogr 154, 121–171.

Frakes, L.A., Francis, J.E., Syktus, J.I., 1992. Climate Modes of the Phanerozoic: the History of the Earth's Climate over the Past 600 Million Years. Clim. Modes Phaneroz. Hist. Earth's Clim. Over Past 600 Million Years. https://doi.org/10.5860/choice.30-6188.

Gulbranson, E.L., Montañez, I.P., Schmitz, M.D., Limarino, C.O., Isbell, J.L., Marenssi, S. A., Crowley, J.L., 2010. High-precision U-Pb calibration of Carboniferous glaciation and climate history, Paganzo Group, NW Argentina. Bull. Geol. Soc. Am. https://doi.org/10.1130/B30025.1.

Gutiérrez, P.R., Limarino, C.O., 2001. Palynology of the Malanzán Formation (upper carboniferous), La Rioja province, Argentina: new data and paleoenvironment considerations. Ameghiniana 38, 98–118.

Harbor, J.N., 1995. Development of glacial-valley cross sections under conditions of spatially variable resistance to erosion. Geomorphology 14, 99–107.

Isbell, J.L., Henry, L.C., Gulbranson, E.L., Limarino, C.O., Fraiser, M.L., Koch, Z.J., Ciccioli, P.L., Dineen, A.A., 2012. Glacial paradoxes during the late Palaeozoic ice age: evaluating the equilibrium line altitude as a control on glaciation. Gondwana Res 22, 1–19.

Isbell, J.L., Miller, M.F., Wolfe, K.L., Lenaker, P.A., 2003. Timing of late Paleozoic glaciation in Gondwana: was glaciation responsible for the development of northern hemisphere cyclothems? Spec. Pap. Geol. Soc. Am. https://doi.org/10.1130/0-8137-2370-1.5.

Jones, M.J., Truswell, E.M., 1992. Late Carboniferous and Early Permian palynostratigraphy of the Joe Joe Group, southern Galilee Basin, Queensland, and implications for Gondwanan stratigraphy. BMR J. Australian Geol. Geoph. 13, 143–185.

Jordan, T.E., Zeitler, P., Ramos, V., Gleadow, A.J.W., 1989. Thermochronometric data on the development of the basement peneplain in the Sierras Pampeanas, Argentina. J. S. Am. Earth Sci. 2, 207–222.

Kar, R.K., Bose, M.N., 1976. Palaeozoic *sporae dispersae* from Zaire (Congo): XII. Assise a couches de houille from Greinerville region. Mus. R. Afr. Cent., Tervuren, Ann. Ser. 8, Sci. Geol. 77, 23–113.

Kneller, B., Milana, J.P., Buckee, C., al Ja'aidi, O., 2004. A depositional record of deglaciation in a paleofjord (Late Carboniferous [Pennsylvanian] of San Juan Province, Argentina): the role of catastrophic sedimentation. Bull. Geol. Soc. Am. https://doi.org/10.1130/B25242.1.

Lele, K.M., Karim, R, 1971. Studies in the Talchir Flora of India. 6. Palynology of the Talchir Boulder Beds in Jayanti Coalfield. Bihar. The Palaeobotanist 19 (1), 52–69.

Limarino, C.O., Alonso-Muruaga, P.J., Ciccioli, P.L., Perez Loinaze, V.S., Césari, S.N., 2014. Stratigraphy and palynology of a late Paleozoic glacial paleovalley in the Andean Precordillera, Argentina. Palaeogeogr. Palaeoclimatol. Palaeoecol. 412, 223–240. https://doi.org/10.1016/j.palaeo.2014.07.030.

Limarino, C.O., Césari, S.N., Net, L.I., Marenssi, S.A., Gutierrez, R.P., Tripaldi, A., 2002. The Upper Carboniferous postglacial transgression in the paganzo and Río Blanco basins (northwestern Argentina): facies and stratigraphic significance. J.S. Am. Earth Sci. 15, 445e460.

Limarino, C.O, Gutierrez, P.R, 1990. Diamictites in the Agua Colorada Formation (northwestern Argentina): new evidence of Carboniferous Glaciation in South America. J. S. Am. Earth Sci. 3, 9–20.

Limarino, C.O., Spalletti, L.A., 2006. Paleogeography of the upper Paleozoic basins of southern South America: an overview. J. South Am. Earth Sci. https://doi.org/10.1016/j.jsames.2006.09.011.

López-Gamundí, O.R., 1997. Glacial-postglacial transition in the late Paleozoic basins of southern South America. In: Martini, I.P.ed. (Ed.), Glacial and Postglacial Environmental Changes, Quaternary, Carboniferous–Permian and Proterozoic. Oxford University Press, Oxford, UK, pp. 147–168.

López-Gamundí, O.R., Buatois, L.A., 2010. Late Paleozoic Glacial Events and Postglacial Transgressions in Gondwana, Late Paleozoic Glacial Events and Postglacial Transgressions in Gondwana. https://doi.org/10.1130/spe468.

López-Gamundí, O.R., Martinez, M., 2000. Evidence of glacial abrasion in the Calingasta-Uspallata and western Paganzo Basins, mid-Carboniferous of western Argentina. Palaeogeogr. Palaeoclimatol. Palaeoecol. 159, 145–165.

Menéndez, C.A., 1965. Contenido palinológico en sendimentos com "Rhacopteris ovata" (Mc Coy) Walkom de La Sierra de Famatina, La Rioja. Revista del Museo Argentino de Ciencias Naturales "Bernardino Rivadavia", Paleontología 1, 45–80.

Milana, J.P., BercowskI, F., 1987. Nueva localidad marina para el Neopaleozoico de Precordi-llera, en la confluencia de los ríos Uruguay y San Juan, Argentina. 4a Reun. Internac. Work. Group PICG-211. (IUGS-UNESCO), S. Cruz de la Sierra, Bolivia, Abstracts, pp. 56–59.

Milana, J.P., Di Pasquo, M., 2019. New chronostratigraphy for a lower to upper Carboniferous strike-slip basin of W-Precordillera (Argentina): paleogeographic, tectonic and glacial importance. J. South Am. Earth Sci. 96, 102383. https://doi.org/10.1016/j.jsames.2019.102383.

Montañez, I.P., Poulsen, C.J., 2013. The late paleozoic ice age: an evolving paradigm. Annu. Rev. Earth Planet Sci. https://doi.org/10.1146/annurev.earth.031208.100118.

Morelli, J., Limarino, C., CésarI, S., Azcuy, C., 1984. Características litoestratigráficas y paleontológicas de la Formación Lagares en los alrededores de la mina Margarita, provincia de La Rioja. IX Congreso Geológico Argentino. San Carlos de Bariloche, Actas IV, pp. 337–347.

Moxness, L.D., Isbell, J.L., Pauls, K.N., Limarino, C.O., Schencman, J., 2018. Sedimentology of the mid-Carboniferous fill of the Olta paleovalley, eastern Paganzo Basin, Argentina: implications for glaciation and controls on diachronous deglaciation in western Gondwana during the late Paleozoic Ice Age. J. South Am. Earth Sci. https://doi.org/10.1016/j.jsames.2018.03.015.

Net, L.I., Alonso, M.S., Limarino, C.O., 2002. Source rock and environmental control on clay mineral associations, lower section of Paganzo group (Carboniferous), northwest Argentina. Sediment. Geol. 152, 183–199.

Noetinger, S., Pujana, R.R., Burrieza, A., Burrieza, H.P., 2017. Use of UV-curable acrylate gels as mounting media for palynological samples. Rev. del Mus. Argentino Ciencias Nat. N.S. 19, 19–23.

Ottone, G.E., 1991. Palinologie du Carbonifere Superieur de la Coupe de Mine La Esperanza, Bassin Paganzo, Argentine. Review du Micropal 34, 118–135.

Pauls, K.N., Isbell, J.L., McHenry, L., Limarino, C.O., Moxness, L.D., Schencman, L.J., 2019. A paleoclimatic reconstruction of the Carboniferous-Permian paleovalley fill in the eastern Paganzo Basin: insights into glacial extent and deglaciation of southwestern Gondwana. J. South Am. Earth Sci. https://doi.org/10.1016/j.jsames.2019.102236.

Playford, G., 1978. Lower Carboniferous spores from the Ducabrook Formation, Drummond Basin, Queensland. Palaeöntographica Abt. B 167, 105–160.

Playford, G., 2015. Mississippian palynolora from the northern Perth Basin, Western Australia: systematics and stratigraphical and palaeogeographical significance. J. Syst. Palaeontol. 14, 731–770.

Potonié, R., Kremp, G., 1955. Die *Sporae dispersae* des Ruhrkarbons, ihre Morphographie und Stratigraphie mit Ausblicken auf Arten anderer Gebiete und Zeitabschnitte, 1. *Palaeöntographica* Abt. B 98, 1–136.

Potonié, R., Lele, K.M., 1961. Studies in the Talchir Flora of India. I. *Sporae dispersae* from the Talchir Beds of South Rewa Gondwana Basin. The Palaeobotanist 8 (1–2), 22–37.

Potonié, R.y., Sah, S.C.D., 1960. *Sporae dispersae* of the lignites from Cannanore Beach on the Malabar Coast of India. The Palaeobotanist 7, 121–135.

Rabassa, J., Carignano, C., Cioccale, M., 2014. A general overview of Gondwana landscpapes in Argentina. In: Rabassa, J., Ollier, C. (Eds.), Gondwana Landscapes in Southern South America: Argentina, Uruguay and Southern Brazil. Springer Earth System Science, Dordrecht, Heidelberg, New York, London, pp. 201–245.

Ramos, V.A., Jordan, T.E., Allmendinger, R.W., Mpodozis, C., Kay, S.M., Corte's, J.M., Palma, M., 1986. Paleozoic terranes of the central Argentine-Chilean Andes. Tectonics 5, 855–880.

Rolleri, E.O., Baldis, B.A.J., 1969. Paleogeography and distribution of carboniferous deposits in the Argentine Precordillera. Coloquio de la IUGS: gondwana stratigraphy, Earth Sciences (2). UNESCO, pp. 1005–1024.

Scotese, C.R., Boucot, A.J., Xu, Chen, 2014. Atlas of Phanerozoic Climatic Zones (Mollweide Projection), Volumes 1-6. *PALEOMAP Project* PaleoAtlas for ArcGIS, PALEOMAP Project, Evanston, IL.

Socha, B., Carignano, C., Rabassa, J., Mickelson, D., 2014. Gondwana glacial paleolandscape, diamictite record of carboniferous valley glaciation, and preglacial remnants of an ancient weathering front in Northwestern Argentina. In: Gondwana Landscapes in Southern South America: Argentina, Uruguay and Southern Brazil. https://doi.org/10.1007/978-94-007-7702-6_12.

Steenken, A., Lopez de Luchi, M.G., Siegesmund, S., Wemmer, K., Pawlig, S., 2004. Crustal provenance and cooling of the basement complexes of the Sierra de San Luis: an insight into the tectonic history of the proto-Andean margin of Gondwana. Gondwana Res. 7, 1171–1195.

Sterren, A.F., Martínez, M., 1996. El Paleovalle de Olta (Carbonífero): Paleoambiente y Paleogeografía. XIII Congreso Geológico Argentino y III Congreso de Exploración de Hidrocarburos, Actas II, pp. 89–103.

Thomas, G.S.P., Connell, R.J., 1985. Iceberg drop, dump, and grounding structures from Pleistocene glacio-lacustrine sediments, Scotland. J. Sediment. Petrol. 55 (2), 243–249.

Tyson, R.V., 1995. Sedimentary Organic Matter. Organic Facies and Palynofacies. Chapman & Hall, Oxford, p. 615.

Utting, J., Wielens, H., 1992. Organic petrology, thermal maturity, geology, and petroleum source rock potential of Lower Permian coal, Karoo Supersystem, Zambia. Energy Sources 14, 337–354.

Valdez, V.B., Aquino, D.C., Paim, P.S.G., Souza, P., Mori, A.L., Fallgatter, C., Milana, J.P., Kneller, B., 2019. Late Palaeozoic glacial cycles and subcycles in western Gondwana: Correlation of surface and subsurface data of the Paraná Basin, Brazil. Palaeogeogr. Palaeoclimatol. Palaeoecol. 531, 108435. https://doi.org/10.1016/j.palaeo.2017.09.004.

Valdez, V.B., di Pasquo, M., Milana, J.P., Kneller, B., Fallgatter, C., Junior, F.C., Gomes Paim, P.S., 2017. Integrated U-Pb zircon and palynological/palaeofloristic age determinations of a Bashkirian palaeofjord fill, Quebrada Grande (Western

Argentina). J. South Am. Earth Sci. 73 https://doi.org/10.1016/j.jsames.2016.12.009.

Valdez, V.B., Milana, J.P., di Pasquo, M., Paim, P.S.G., Philipp, R.P., Aquino, C.D., Cagliari, J., Junior, F.C., Kneller, B., 2020. Timing of the late palaeozoic glaciation in western Gondwana: new ages and correlations from Paganzo and Paraná basins. Palaeogeogr. Palaeoclimatol. Palaeoecol. 544 https://doi.org/10.1016/j.palaeo.2020.109624.

Veevers, J.J., Powell, C.M., 1987. Late Paleozoic glacial episodes in Gondwanaland reflected in transgressive- regressive depositional sequences in Euramerica. Geol. Soc. Am. Bull. https://doi.org/10.1130/0016-7606(1987)98<475:LPGEIG>2.0.CO;2.